

## Review Article

# The basis of anisotropic water diffusion in the nervous system – a technical review

Christian Beaulieu\*

Department of Biomedical Engineering, Faculty of Medicine, University of Alberta, Edmonton, Alberta, Canada

Received 5 June 2001; Revised 12 October 2001; Accepted 16 October 2001

**ABSTRACT:** Anisotropic water diffusion in neural fibres such as nerve, white matter in spinal cord, or white matter in brain forms the basis for the utilization of diffusion tensor imaging (DTI) to track fibre pathways. The fact that water diffusion is sensitive to the underlying tissue microstructure provides a unique method of assessing the orientation and integrity of these neural fibres, which may be useful in assessing a number of neurological disorders. The purpose of this review is to characterize the relationship of nuclear magnetic resonance measurements of water diffusion and its anisotropy (i.e. directional dependence) with the underlying microstructure of neural fibres. The emphasis of the review will be on model neurological systems both *in vitro* and *in vivo*. A systematic discussion of the possible sources of anisotropy and their evaluation will be presented followed by an overview of various studies of restricted diffusion and compartmentation as they relate to anisotropy. Pertinent pathological models, developmental studies and theoretical analyses provide further insight into the basis of anisotropic diffusion and its potential utility in the nervous system. Copyright © 2002 John Wiley & Sons, Ltd.

**KEYWORDS:** diffusion; anisotropy; nerve; white matter; spinal cord; water; MRI; DTI

## INTRODUCTION

All diffusion-tensor magnetic resonance imaging (DTI) studies of nerve, spinal cord white matter and brain white matter rely on the underlying phenomenon that water diffusion is highly anisotropic in these tissues of the nervous system. A basic understanding of the influence of various structural components on anisotropic water diffusion is a prerequisite for interpreting alterations in diffusion and anisotropy as a result of various disease processes or abnormal development. The purpose of this article is to provide an overview of this fundamental property of water as it relates to the non-invasive interrogation of neural fibre composition, integrity and orientation, studies which are

not possible with other imaging methods. The article will focus on published reports that have used *in vitro* and *in vivo* neurological model systems to characterize the dependency of water diffusion on the underlying microstructure of the fibre tracts. After some introductory paragraphs on defining anisotropic diffusion, the early observations of anisotropy in the nervous system will be covered as well as some detailed investigations of the contributions of various structural components to anisotropy. A discussion of restricted diffusion and diffusion in the various neural compartments as it relates to the absolute measures of diffusion and their anisotropy will be attempted in this rather complex and controversial field. Further insights into the basis of anisotropic water diffusion and the utility of this novel water property in biology and medicine then follow from a synopsis of detailed basic studies on pathology, development and computer modelling of diffusion in neural fibres. Clinical studies utilizing anisotropy will not be covered unless they are directly relevant to a specific point brought up in this review since they are the subject of more detailed reviews by others in this special issue.

## ISOTROPIC VS ANISOTROPIC DIFFUSION

Diffusion is a physical process that involves the

\*Correspondence to: C. Beaulieu, Department of Biomedical Engineering, 1098 Research Transition Facility, University of Alberta, Edmonton, Alberta, Canada T6G 2V2.

Email: christian.beaulieu@ualberta.ca

Contract/grant sponsor: Alberta Heritage Foundation for Medical Research.

Contract/grant sponsor: Canadian Institutes of Health Research.

**Abbreviations used:** ADC, apparent diffusion coefficient; *b*, gradient factor; *D*, diffusion coefficient; DTI, diffusion-tensor imaging; DWI, diffusion-weighted imaging; EAE, experimental allergic encephalomyelitis; *G*, strength of diffusion gradients; PGSE, pulsed-gradient spin-echo; RMS, root mean square displacement; SNR, signal-to-noise ratio; *T*<sub>2</sub>, transverse relaxation time; *t*<sub>dif</sub>, diffusion time; *TE*, spin-echo time; ||, parallel to the fibre's long axis; ⊥, perpendicular to the fibre's long axis;  $\delta$ , length of diffusion gradient;  $\Delta$ , onset separation of diffusion gradients;  $\lambda$ , principal eigenvalues.

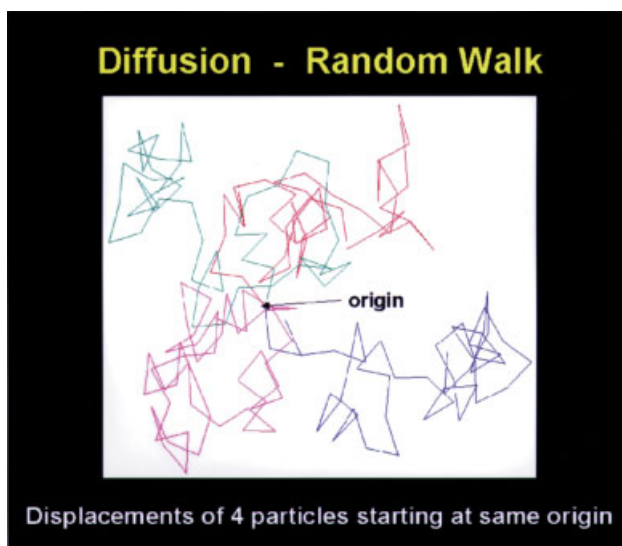


**Figure 1.** Diffusion is a process which can best be described as a random walk. Four particles, indicated by different colours, all begin at the same origin yet follow different chaotic paths. In tissue, the diffusion paths of the particles, e.g. water molecules, will be influenced by cellular microstructures which can impede the translational mobility of the diffusing particles

translational movement of molecules via thermally driven random motions, so-called Brownian motion (Fig. 1). The mobility of the molecules can be characterized by a physical constant dubbed the diffusion coefficient,  $D$ , which is related to the root mean square displacement, RMS, of the molecules over a given time,  $t_{\text{dif}}$ , via the Einstein equation [one-dimensional RMS =  $(2D t_{\text{dif}})^{1/2}$ ]. The factors influencing diffusion in a solution (or self-diffusion in a pure liquid) are molecular weight, intermolecular interactions (viscosity), and temperature. The underlying cellular microstructure of tissue complicates the situation and influences the overall mobility of the diffusing molecules by providing numerous barriers and by creating various individual compartments (e.g. intracellular, extracellular, neurons, glial cells, axons) within the tissue. The diffusion coefficient measured by nuclear magnetic resonance (NMR) is best known in the biological NMR literature as the *apparent* diffusion coefficient (ADC) to take into account that it is not a true measure of the 'intrinsic' diffusion, but rather that it depends on the interactions of the diffusing molecule, in most cases water, with the cellular structures over a given diffusion time. The apparent diffusion could also potentially be influenced by active processes within the tissue. Only over very short diffusion times will the measured diffusivity of the molecules reflect the local intrinsic viscosity, whereas at longer diffusion times the effects of the barriers become apparent. The former case is not usually achievable in practice at present because of the small dimensions of individual compartments in tissue (on the order of  $\mu\text{m}$ ) and in fact we take advantage of the latter

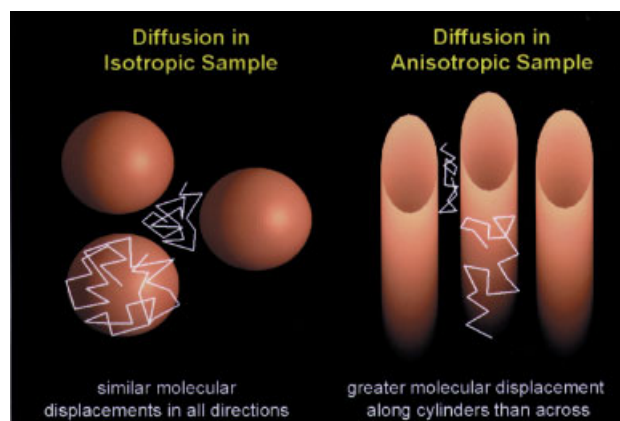


**Figure 2.** An illustration depicting diffusion in two different types of samples, one which has similar molecular displacements in all directions (isotropic diffusion) and the other which has greater diffusion along one direction over another (anisotropic diffusion). The surfaces are impermeable in this cartoon for illustrative purposes only

case by permitting enough time for the diffusing molecules to sample the local environment and then infer microstructural characteristics of the tissue from the measured diffusion properties.

The distance that a molecule diffuses in one direction in space may or may not be the same as in some other direction. Clearly, in a pure liquid where there are no hindrances to diffusion or in a sample where the barriers are not coherently oriented, diffusion is the same in all directions and is termed *isotropic* diffusion. However, if diffusion depends on direction, like in a sample with highly oriented barriers, it is termed *anisotropic* diffusion. In this way, structural subtypes can be identified simply on the basis of their diffusion characteristics (Fig. 2) and the anisotropy is directly related to the geometry of the fibres. The degree of hindrance to water diffusion will be determined by the size, shape and composition of any physical obstructions, as well as the spacing between those obstructions. Diffusion can be evaluated by measuring the signal intensity ( $I$ ) attenuation as a function of the so-called diffusion-sensitizing 'gradient factor', i.e.  $b$  value, which are related via  $I = I_0 e^{-bD}$ . The  $b$  value is a function of the gyromagnetic ratio of the nucleus of interest as well as the gradient strength and timings of the diffusion-sensitizing gradients. Therefore, a plot of  $\ln(I/I_0)$  vs  $b$  value in a single component, unrestricted system will be linear with the slope yielding a measure of  $D$ , the diffusion coefficient. Celery has often been used as a model system for illustrative purposes, since it demonstrates isotropic diffusion in the parenchyma ('bulk'), i.e. equal diffusion in all directions, and anisotropic water diffusion in the vascular bundles ('strings'), i.e. diffusion parallel to the bundles is much greater than perpendicular (Fig. 3).<sup>1,2</sup> The greater signal attenuation along the direction parallel to the long axis of

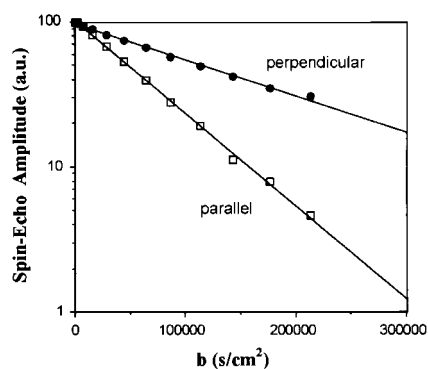


**Figure 3.** Diffusion curves of water in vascular bundles of celery measured parallel and perpendicular to their long axis. Larger molecular displacements parallel to the bundles cause greater attenuation of the echo relative to the perpendicular direction which signifies marked anisotropic diffusion. The ADC values parallel and perpendicular to the celery vascular bundles are  $1.47 \times 10^{-5} \text{ cm}^2 \text{ s}^{-1}$  and  $0.64 \times 10^{-5} \text{ cm}^2 \text{ s}^{-1}$ , respectively, at room temperature (20–25 °C)

the celery vascular bundles relative to the perpendicular direction for the same  $b$  value reflects larger molecular displacements along the parallel axis which is indicative of anisotropy. In fact, the anisotropic diffusion ratios  $[\text{ADC}(\parallel)/\text{ADC}(\perp)]$  obtained were  $1.0 \pm 0.1$  and  $2.3 \pm 0.4$  for celery parenchyma and vascular bundles, respectively.<sup>3</sup> This observation is not surprising since the cells in the parenchyma are generally isodiametric and hence impart equal barriers to diffusion in all directions, whereas those in the vascular bundles are elongated and longitudinally oriented.

Magnetic resonance measurements of diffusion are sensitive to molecular displacements along the axis of the diffusion-sensitizing gradients applied in a standard Stejskal–Tanner pulsed-gradient spin-echo (PGSE) experiment.<sup>4</sup> Therefore, diffusion along different directions in tissue can be readily evaluated by varying the direction (i.e. axis) of the diffusion-sensitizing gradients. This review will not attempt to cover the techniques involved in measuring the ADC, nor will it expand on the virtues of the diffusion tensor and the various methods of quantifying anisotropy.<sup>5–8</sup> In many of the discussions outlined below, excised neural fibre samples could be readily oriented parallel or perpendicular to the applied gradients (i.e. the laboratory frame) in order to simplify the measurements of the principal diffusion coefficients. Although it is certainly not the most sophisticated measure of anisotropy, the ratio of the parallel ADC over the perpendicular ADC is presented in several examples in this review since it was used in many of the early studies, the fibre frame and the laboratory frame were aligned which obviated the need for acquiring the full tensor, the SNR was good (helped in providing adequate statistical stability), and it can provide an immediate, intuitive feel for the degree of anisotropy.

## EARLY OBSERVATIONS

In the late 1960s and early-to-mid 1970s there was great interest in understanding the state of ions and water in cytoplasm. The ADC of ions and water in tissue were reduced typically by a factor of 2–5 in comparison to the ADC in bulk water, with the translational diffusion of water in excised brain hindered to a greater extent than in excised muscle.<sup>9,10</sup> Slight anisotropic water diffusion was observed in excised rat skeletal muscle, i.e. water diffusion was greater parallel ( $\parallel$ ) to the length of the fibres than perpendicular ( $\perp$ )  $[\text{ADC}(\parallel)/\text{ADC}(\perp) \approx 1.4]$ .<sup>11</sup> The phenomenon of anisotropic diffusion was well known in the chemistry arena such as in studies of liquid crystals, etc.<sup>12</sup> A resurgence of diffusion studies in biology and medicine was sparked in the mid-1980s by the advent of diffusion-weighted magnetic resonance imaging (DWI) which could be used to measure diffusion coefficients in various tissues *in vivo*. The idea of measuring anisotropic diffusion in tissue fibres in humans was pointed out in one of the first papers on DWI.<sup>13</sup>

Early measurements of water diffusion in normal human brain white matter *in vivo* by Thomsen *et al.* showed large variations of the ADC.<sup>14</sup> They proposed that the regional differences in diffusion could be from anisotropic diffusion due to the orientation of the myelin sheaths in the white matter tracts. In other words, the water molecules would preferentially diffuse along the length of the axons and would be hindered by barriers such as the myelin sheath when diffusing perpendicular to the axons. Therefore, depending on the relative orientation of the applied diffusion-sensitizing gradients and the white matter tracts, a spread of ADC values could be measured in white matter. Grey matter, on the other hand, does not have an oriented fibre structure and thus would not be expected to exhibit anisotropic diffusion.\* Others subsequently observed a directional dependence of DWI contrast and the ADC in the white matter of the human brain.<sup>19–22</sup>

The first systematic study of anisotropic water diffusion in the nervous system by Moseley *et al.* confirmed that water diffusion was anisotropic in normal white matter of cat brain and spinal cord whereas diffusion was isotropic in grey matter.<sup>23</sup> Anisotropy was observed also in human spinal cord,<sup>24</sup> human sciatic nerve,<sup>24</sup> human tibial nerve,<sup>25</sup> cat optic nerve,<sup>25</sup> peripheral nerves in the rabbit forelimb,<sup>26</sup> and rat trigeminal nerve and corpus callosum *in vivo*.<sup>2,27</sup> The parallel and perpendicular ADC values were around  $0.9$ – $1.3 \times 10^{-5} \text{ cm}^2 \text{ s}^{-1}$  and  $0.3$ – $0.5 \times 10^{-5} \text{ cm}^2 \text{ s}^{-1}$ , respectively. The degree of anisotropy, as given by the ratio of  $\text{ADC}(\parallel)$  to  $\text{ADC}(\perp)$ , was  $\sim 2$ – $4$  when measured over typical diffusion times  $\sim 20$ – $40$  ms and was quite similar

\*Grey matter in the rat cortex<sup>15–17</sup> and neonatal piglet cortex<sup>18</sup> actually demonstrates a small degree of diffusion anisotropy presumably due to the radiating pattern of the pyramidal cells.

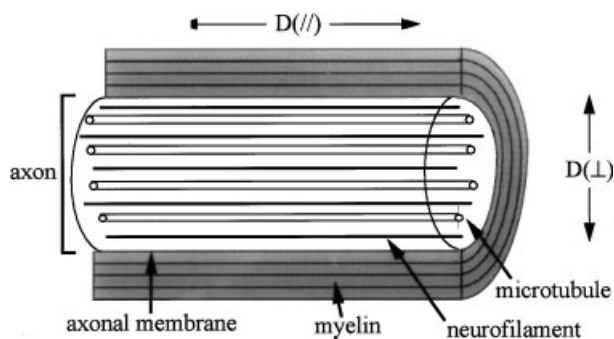


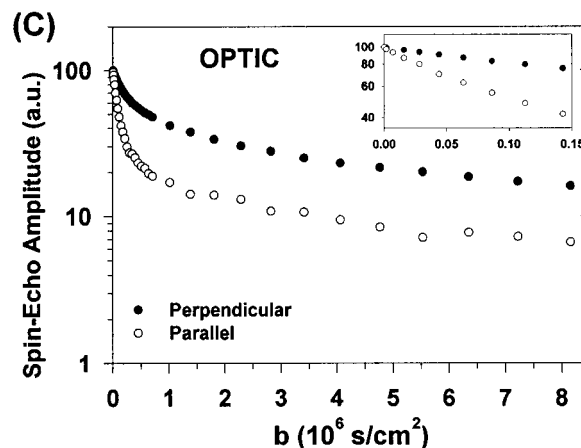
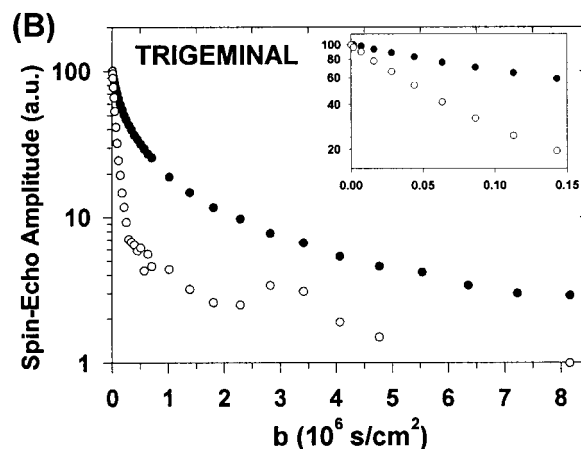
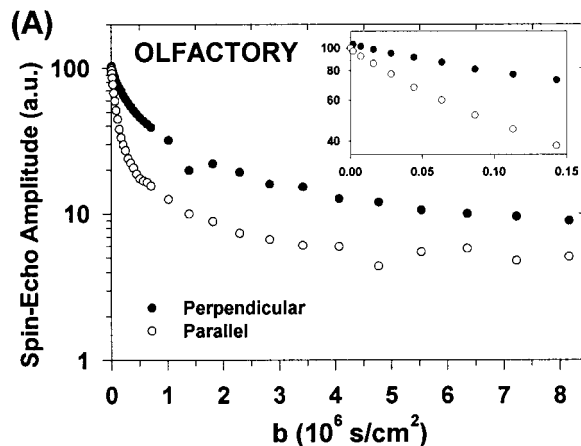
**Figure 4.** A simplistic schematic of the longitudinal view of a myelinated axon. Myelin, the axonal membrane, microtubules, and neurofilaments are all longitudinally oriented structures that could hinder water diffusion perpendicular to the length of the axon and cause the perpendicular diffusion coefficient,  $D(\perp)$  to be smaller than the parallel diffusion coefficient,  $D(\parallel)$ . Other postulated sources of diffusion anisotropy are axonal transport and susceptibility-induced gradients

despite the variety of fibre types and species. Furthermore, the anisotropy was significantly greater than that observed in muscle. Some of the first studies recognized the value of measures of diffusion anisotropy for following brain maturation<sup>28,29</sup> or mapping fibre orientation in the brain non-invasively.<sup>30</sup> Reviews in 1991 by two pioneers in the field of NMR measurements of water diffusion in biological systems, Michael Moseley and Denis Le Bihan, provide further details on the early views of diffusion.<sup>1,31</sup> As both authors pointed out, although diffusion taking the path of least resistance along the oriented fibres was an obvious and plausible explanation for the observed anisotropy, the specific origin of anisotropic water diffusion was still unknown and unevaluated in the neural fibre tracts.

**Figure 5.** Representative diffusion decay curves for (A) the non-myelinated olfactory nerve, (B) the Schwann cell myelinated trigeminal nerve, and (C) the oligodendrocyte myelinated optic nerve of the garfish are presented over a large range of  $b$  values up to  $\sim 8 \times 10^6 \text{ s cm}^{-2}$  (i.e.  $80\,000 \text{ s mm}^{-2}$ ). The perpendicular (solid circles) and parallel (open circles) measurements refer to the long axis of the nerve fibres and demonstrate similar degrees of anisotropy in all three very different nerves. This was one of the first conclusive pieces of evidence to suggest that myelin was not a necessary determinant for anisotropic water diffusion in neural fibres. Given the need for powerful gradients, the observation of non-monoexponential decay of signal along both axes in the garfish nerves was one of the first reports of this phenomenon in neural fibres. The perpendicular curves level off at a higher amplitude than the parallel curves at high  $b$  values for a given nerve. The inset plots demonstrate the diffusion curves at low  $b$  values typical of clinical MRI studies. The figures have been adapted from data presented in Beaulieu and Allen.<sup>34</sup>

## POSTULATED SOURCES AND INVESTIGATION OF DIFFUSION ANISOTROPY

Anisotropic water diffusion is no doubt related to the ordered arrangement of the myelinated fibres in nerve and white matter. However, little work had been performed to determine the relative contributions of the various structural components of white matter to the



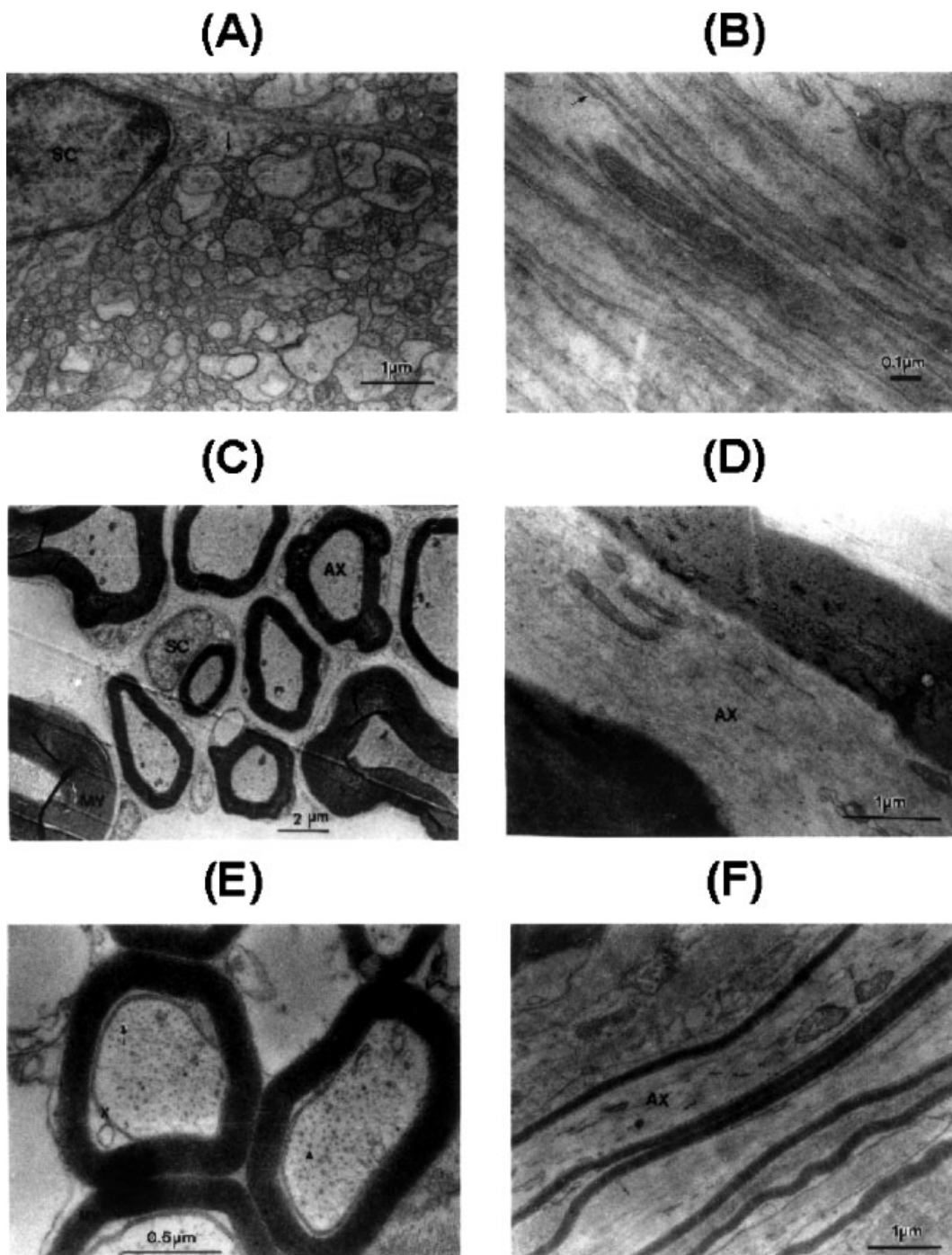
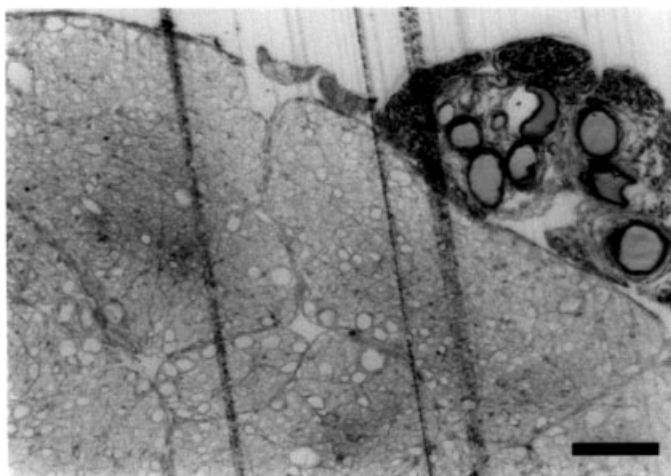


**Figure 6.** Electron micrographs of transverse (A, C, E) and longitudinal (B, D, F) sections from freshly excised non-myelinated olfactory (A, B), myelinated trigeminal (C, D), and myelinated optic (E, F) nerves of the garfish. *Olfactory nerve*: (A) The small ( $\sim 0.25 \mu\text{m}$  diameter), circular, relatively homogeneous non-myelinated axons (arrow) are packed together tightly. Microtubules (seen as small dots within the axons) and a Schwann cell nucleus (SC) are visible. (B) Axonal membranes (arrow) run diagonally across the micrograph. *Trigeminal nerve*: (C) The axons (AX) have diameters  $\sim 3\text{--}6 \mu\text{m}$  and appear to have good circular shapes which is indicative of a structurally sound nerve. Furthermore, the myelin sheaths (MY) are intact. In peripheral nerves, axons are myelinated by Schwann cells (SC). (D) Numerous longitudinal filaments are visible within an axon (AX). *Optic nerve*: (E) The cytoskeletal elements, namely microtubules (arrowhead) and neurofilaments (arrow), are visible within the intact axons ( $\sim 1 \mu\text{m}$  diameter). Microtubules have a doughnut-shaped cross-section and are  $\sim 25 \text{ nm}$  in diameter, whereas neurofilaments do not have a hollow central core and are only  $\sim 10 \text{ nm}$  in diameter. The multi-lamellar nature of the myelin sheath (MY) is evident. The axonal membrane ( $\times$ ) is also visible. (F) The longitudinal structure of the nerve is evident as three myelinated axons (AX) traverse diagonally across the micrograph

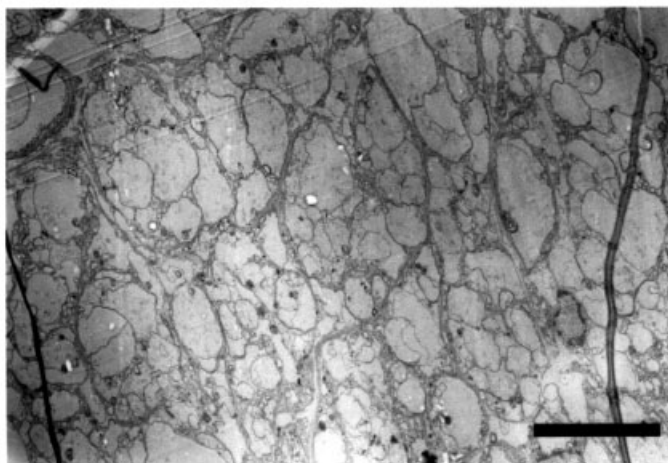
anisotropy of the water diffusion coefficients. Nonetheless, several possible origins of anisotropy had been postulated. For our purposes, and to simplify the discussion, nerves (peripheral, central) and white matter

(spinal cord, brain) are all ordered axonal systems which consist of essentially the same primary microstructural components. The myelin sheath around the axons, the axonal membrane and the neurofibrils (microtubules,

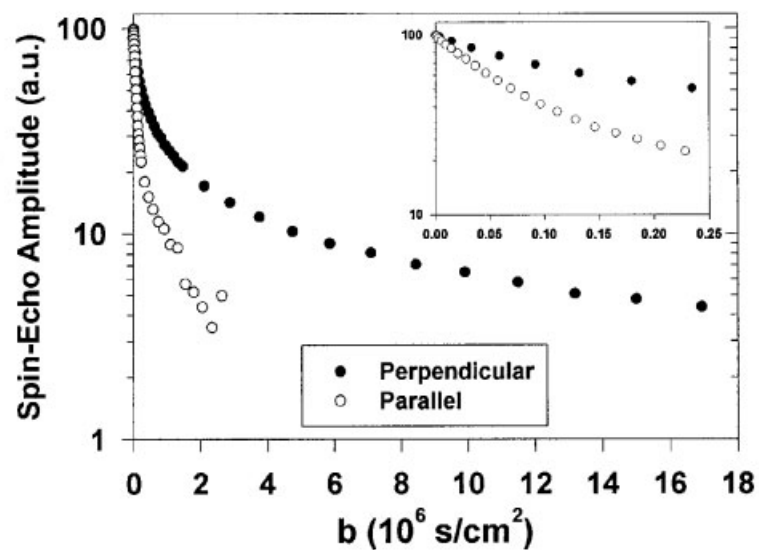
(A)



(B)



(C)



neurofilaments) are three longitudinally oriented structures that could impart non-random barriers to diffusion (Fig. 4) and hence reduce diffusion perpendicular to the fibres,  $ADC(\perp)$ , with respect to diffusion parallel,  $ADC(\parallel)$ . Alternatively, some have proposed that the diffusion parallel to the length of the axons could be accentuated by axonal transport. Others have suggested that water diffusion, as measured by NMR, could be anisotropic due to local susceptibility-difference-induced gradients in the nerves and white matter.<sup>32,33</sup>

## Myelin and axonal membranes

The preferred, but unproven, hypothesis of the time for anisotropic water diffusion was the hindrance of perpendicular water diffusion by the myelin sheath encasing the axons, which was understandable given the interest in pursuing studies on white matter maturation and demyelinating disease such as multiple sclerosis. The numerous lipid bilayers of myelin have limited permeability to water and would be expected to hinder diffusion across the fibres, particularly the axonal water, relative to the length of the axons where such barriers did not exist. If myelin were the sole source of anisotropy, then it was naively expected that diffusion would be much more isotropic in a normal fibre tract without myelin. In one of the first systematic studies on the underlying source of anisotropy, this was found not to be the case by Beaulieu and Allen, who showed that water diffusion was significantly anisotropic in a normal, intact, non-myelinated olfactory nerve of the garfish (Fig. 5).<sup>34</sup> The degree of anisotropy in the non-myelinated olfactory nerve [ $ADC(\parallel)/ADC(\perp)=3.6$ ] was similar to that observed in the garfish trigeminal nerve myelinated with Schwann cells [ $ADC(\parallel)/ADC(\perp)=3.2$ ] and the garfish

optic nerve myelinated with oligodendrocytes [ $ADC(\parallel)/ADC(\perp)=2.6$ ]; (Fig. 5). The degree of anisotropy in these excised nerve samples measured at room temperature was quite similar to the anisotropy measured *in vivo* in humans, lending credibility to the *in vitro* data, although the absolute ADC values were likely modulated by the excision of the nerves and the temperature difference. Although it will be discussed in more detail later on, one important observation was the clear non-linearity of the diffusion decay curves for these garfish nerves (Fig. 5). Since there have been several incorrect citations of that earlier paper, it is important to note that the garfish olfactory nerve is normally non-myelinated and is *not* a model of demyelination. Representative transverse and longitudinal electron micrographs of the garfish olfactory, trigeminal, and optic nerves are presented in Fig. 6 and highlight the important structural features in neural fibres. This study provided the first unequivocal evidence that myelin was not an essential component for anisotropic diffusion in neural fibres. This is *not* to say that myelin does not play a role in anisotropy, but rather this observation serves to point out that structural features of the axons other than myelin are *sufficient* to give rise to anisotropy and that interpretations of changes in anisotropy with respect to just myelination must be made with caution.

The initial observation of anisotropy in the intact non-myelinated garfish olfactory nerve has subsequently been confirmed in various other models with non-myelinated neural fibres both *in vitro* and *in vivo*. Previously unpublished diffusion measurements of water in the *non-myelinated* walking leg nerves of the lobster are presented in Fig. 7. Significant anisotropy is observed over the full range of  $b$  values investigated (up to  $18\,000\,000\text{ s cm}^{-2}$  or  $180\,000\text{ s mm}^{-2}$ ). The single component ADC values obtained at low  $b$  values (i.e.  $\leq 1 \times 10^5\text{ s cm}^{-2}$ ) were  $1.12 \times 10^{-5}\text{ cm}^2\text{ s}^{-1}$  and  $0.41 \times 10^{-5}\text{ cm}^2\text{ s}^{-1}$  parallel and perpendicular to the nerve axis, respectively. The absolute ADC values and their anisotropy [ $ADC(\parallel)/ADC(\perp)=2.8$ ] in the non-myelinated walking leg nerve of the lobster are in the range of the previously reported non-myelinated and myelinated nerves of the garfish.<sup>34</sup> Clearly, the packed arrangement of non-myelinated axons<sup>35</sup> is sufficient to impede perpendicular water diffusion and generate anisotropy (Fig. 7). Wimberger *et al.* and Prayer *et al.* demonstrated that diffusion became anisotropic in the white matter of rat pups prior to histological evidence of myelination and much earlier than changes on  $T_2$ -weighted images.<sup>36,37</sup> The 2 week old 'jumpy' mouse had persistent diffusion anisotropy in the optic nerve relative to age-matched controls despite the absence of myelination (axons are preserved), although the degree of anisotropy was relatively low in both cases.<sup>38</sup> Significant anisotropy was observed in the non-myelinated vagus nerve of the rat.<sup>39</sup>

A recent report by Gulani *et al.* of diffusion tensor

**Figure 7.** Previously unpublished diffusion measurements of water in the excised, *non-myelinated* walking leg nerve of the lobster. (A) Light micrograph of a portion of a transverse section of the lobster nerve demonstrating numerous smaller, non-myelinated axons and a handful of larger axons (~30–50  $\mu\text{m}$ ) with a few Schwann cell wrappings (top right corner). The black bar in the bottom right corner represents 100  $\mu\text{m}$ . (B) Transverse electron micrograph of several non-myelinated axons with diameters ranging from 3 to 8  $\mu\text{m}$  located in the central portion of the nerve. The black bar in the bottom right corner represents 10  $\mu\text{m}$ . (C) Stejskal–Tanner PGSE measurements of water diffusion ( $\delta = 6\text{ ms}$ ,  $\Delta = 30\text{ ms}$ , diffusion time = 28 ms constant as gradient strength varied) obtained at 20 °C at a static magnetic field strength of 2.35 T (similar to the garfish nerve measurements in Beaulieu and Allen<sup>34</sup>). Significant anisotropy in the signal attenuation curves is evident over a very large range of  $b$  values (up to  $18\,000\,000\text{ s cm}^{-2}$  or  $180\,000\text{ s mm}^{-2}$ ). Marked deviations from mono-exponential decay are observed when the diffusion-sensitizing gradients are applied either parallel or perpendicular to the long axis of nerve. The inset plot demonstrates the diffusion curves at low  $b$  values

micro-imaging of the spinal cord in the myelin-deficient rat, an X-linked recessive Wistar rat mutant which shows near total lack of myelination in its central nervous system, has resulted in some very interesting findings.<sup>40</sup> First, they convincingly corroborated the finding that myelination of white matter is not a requirement for the presence of significant anisotropic diffusion. In keeping with the ratio of parallel and perpendicular ADCs that we have been using thus far in this article, the anisotropic diffusion ratio was  $\sim 4.5$  and  $\sim 3.5$  in the control and myelin deficient white matter, respectively (or  $A_{\sigma} \approx 0.53$  and  $0.45$  with their measure of anisotropy). The anisotropy decreased only by  $\sim 20\%$  in the myelin-deficient rats and signified that the residual structures, namely the membranes of the numerous axons, are sufficient for significant anisotropic diffusion in this model. However, the absence of myelin did alter the absolute ADC values. The mean or 'trace' diffusivity increased by  $\sim 50\%$  from  $0.37 \times 10^{-5} \text{ cm}^2 \text{ s}^{-1}$  to  $0.55 \times 10^{-5} \text{ cm}^2 \text{ s}^{-1}$ . This increased water mobility was more prevalent in the perpendicular direction (ADC increased by  $\sim 75\%$ ) than in the parallel direction (ADC increased by  $\sim 35\%$ ), as might be expected with the loss of myelin. In addition to animal studies, *in vivo* human measurements in neonates by Hüppi *et al.* and Neil *et al.* have shown diffusion anisotropy in non-myelinated fibres of the corpus callosum<sup>41</sup> or anterior limb of the internal capsule.<sup>42</sup> Anisotropic water diffusion in neural fibres must not be regarded as myelin specific. Axonal membranes play a major role since, as we will see below, the other potential contributors (neurofibrils, fast axonal transport, susceptibility) to anisotropy are not significant.

However, the study by Gulani *et al.* also demonstrated that myelination can *modulate* the degree of anisotropy.<sup>40</sup> In general though, a quantitative or even qualitative determination of the relative importance of myelin, relative to the axonal membranes, for anisotropy in a given fibre tract is difficult to assess. Direct comparisons of anisotropy between unique fibres with different axon diameters, degree of myelination, and fibre packing density are fraught with difficulty. For example, the non-myelinated olfactory nerve of the garfish actually has a higher degree of anisotropy than the myelinated trigeminal and optic nerves of the garfish.<sup>34,43</sup> Since the axonal diameters are an order of magnitude smaller in the olfactory nerve, it is difficult to get a handle on the relative contribution of myelin to the anisotropy in the trigeminal and optic nerves. Rudimentary estimates of the numbers of membranes (as the axonal membrane or myelin wrappings) 'encountered' over a typical 1D-RMS displacement perpendicular to the fibre axis were similar in range (30–70 membranes) for all three of these nerves.<sup>34</sup> This suggests that membrane density may play a role, but it is clearly an oversimplification of the biological complexity given the variability in axon dimensions, thickness of myelin, extracellular spacing

between axons, variable membrane permeabilities, exchange, etc.

Nonetheless, for two given fibre tracts with equally sized axons and density (i.e. spacing), one with myelin and one without myelin, we would still predict that myelin would likely increase anisotropy by a certain, albeit unknown, extent due to greater hindrance to intra-axonal diffusion and greater tortuosity for extra-axonal diffusion. Pierpaoli *et al.* also had difficulty in attributing particular microstructural features (e.g. packing density) to explain the variable degrees of diffusion anisotropy observed amongst different white matter tracts in the adult human brain.<sup>44</sup> Anisotropy is observed to increase with development,<sup>29</sup> although there are questions as to whether this signifies myelination and/or just improved coherence of the fibre tracts. These issues related to developmental or pathological studies will be discussed later in this review. At this stage, the contributions of several other anisotropy candidates need to be investigated.

### Neurofibrils and fast axonal transport

The complex and dense three-dimensional cytoskeleton of axons is mainly composed of longitudinally oriented, cylindrical neurofibrils, namely microtubules and neurofilaments, which are inter-connected by small microfilaments. These structures could presumably cause anisotropic diffusion if the small, but numerous, neurofibrils presented sufficient physical barriers to hinder perpendicular water diffusion to a greater extent than parallel. In addition to providing physical obstruction, fast axonal transport is intimately linked to the presence of microtubules since cellular organelles (e.g. mitochondria, vesicles) are transported by their attachment to mechanochemical enzymes that pull the organelles along the microtubule tracks.

The role of microtubules and fast axonal transport in anisotropic diffusion was evaluated in excised myelinated and non-myelinated nerves of the garfish that were treated with vinblastine, which is known to depolymerize microtubules and inhibit fast axonal transport.<sup>34</sup> The authors demonstrated that anisotropy was preserved in all three types of nerve treated with vinblastine suggesting that microtubules, of themselves, and the fast axonal transport they facilitate are not the dominant determinants of anisotropy. However, all three vinblastine-treated nerves demonstrated absolute ADC decreases of  $\sim 30\text{--}50\%$  in both the parallel and perpendicular directions relative to the freshly excised nerves which were attributed to either an increase in free tubulin (the monomeric unit of microtubules), the presence of vinblastine paracrystals within the axoplasm, or some degradation over the 48 h that the nerves were immersed in buffer containing vinblastine.

This earlier study did not assess the role of the



numerous longitudinally oriented neurofilaments, the primary structural component of the axoplasm. Beaulieu and Allen evaluated the influence of the neurofilamentary cytoskeleton on water mobility by making measurements in axoplasm with minimal interference from membranes.<sup>45</sup> The isolated giant axon from squid was used because it can provide an axoplasmic space (diameter  $\sim 200\text{--}1000\ \mu\text{m}$ ) whose dimension is much greater than the one-dimensional, root-mean-square displacement ( $\sim 11\ \mu\text{m}$ ) of a water molecule randomly diffusing over typical diffusion times used in NMR studies ( $\sim 30\ \text{ms}$ ). The diffusion coefficients of water parallel and perpendicular to the long axis of the squid giant axon at  $20^\circ\text{C}$  were  $1.6 \times 10^{-5}\ \text{cm}^2\ \text{s}^{-1}$  and  $1.3 \times 10^{-5}\ \text{cm}^2\ \text{s}^{-1}$ , respectively, which yielded an anisotropic diffusion ratio ( $\parallel/\perp$ ) of 1.2. This experimental measure of anisotropy matched Monte Carlo computer simulations of randomly diffusing particles in a regular, hexagonal array of circular barriers whose size (10 nm) and spacing (20–60 nm) were chosen to simulate the neurofilamentary lattice.<sup>45</sup> Two important findings resulted from this work. First, the neurofilaments do not have a significant role in producing diffusion anisotropy within the axon and thus pointed towards the importance of membranes, either in the form of myelin or multiple axonal membranes, in fulfilling the role as the primary determinant of the observed anisotropy in neural fibres. Second, water diffusion in pure axoplasm is rapid and is  $\sim 70\text{--}80\%$  of that in pure water at  $20^\circ\text{C}$  ( $\text{ADC} \sim 2 \times 10^{-5}\ \text{cm}^2\ \text{s}^{-1}$ ). This latter point will be further discussed when we consider compartmental issues and diffusion.

### Susceptibility

Anisotropic water diffusion, as measured by NMR, could be due to local susceptibility-difference-induced gradients in the nerves and white matter.<sup>32,33</sup> The first evaluation of its potential contribution to white matter was performed by Trudeau *et al.* on excised porcine spinal cord at 4.7 T.<sup>46</sup> By varying the orientation of the fibre tracts parallel or perpendicular to the static magnetic field ( $B_0$ ), the background gradients could be minimized or maximized, respectively. The ADCs parallel or perpendicular to the fibres measured with the standard PGSE diffusion sequence were independent of the fibre orientation relative to  $B_0$  and hence the induced gradients do not play a role in the anisotropy of diffusion in white matter. They also used a bipolar gradient pulse sequence to eliminate the effect of the background gradients on the ADC values, but the interpretation of their data was complicated by the difference in diffusion time relative to the standard PGSE sequence. The ADC and anisotropy independence on susceptibility-induced gradients was subsequently confirmed by Beaulieu and Allen in four different excised nerves from garfish and frog at 2.35 T by varying the orientation of the fibres relative to the

static magnetic field and by eliminating the background gradients through the use of a spin-echo diffusion sequence with a specific bipolar gradient pulse scheme.<sup>43</sup> Clark *et al.* extended this result to human brain white matter *in vivo* at 1.5 T.<sup>47</sup>

### Summary

Anisotropic water diffusion is clearly not unique to neural fibre tracts (it is even seen in salt water ice<sup>48</sup>) and is observed in other tissues such as kidney, skeletal muscle, and myocardium;<sup>11,49,50</sup> however, the degree of anisotropy tends to be much less than that found in neural fibre tracts. By experimentally eliminating a dominating role for fast axonal transport, the axonal cytoskeleton of neurofilaments and microtubules, and local susceptibility-difference-induced gradients, intact membranes are confirmed to be the primary determinant of anisotropic water diffusion in neural fibres such as brain or spinal cord white matter and nerve. The available data do not permit the dissection of the individual contributions of myelin and axonal membranes to the degree of anisotropy, but the evidence suggests that axonal membranes play the primary role and that myelination, although not necessary for significant anisotropy, can modulate the degree of anisotropy. Analytical modelling and computer simulations, which will be presented later in the article, help to confirm the role of membranes as the primary barriers to perpendicular water diffusion.

### RESTRICTED DIFFUSION AND COMPARTMENTAL ISSUES RELATED TO ANISOTROPY

As mentioned in the last section, the diffusion perpendicular to neural fibres is influenced, i.e. reduced, by interactions of the diffusing water molecules with the numerous membranes. If the water molecules no longer move freely, they are said to undergo *restricted diffusion*. Hindered diffusion may be a more appropriate term for biological systems since membranes certainly have a finite permeability for water. The variation of the diffusion decay curves and the measured ADC with the diffusion time are hall-marks of restricted diffusion.<sup>51,52</sup> The molecules will experience fewer boundaries and display diffusion behaviour closer to free diffusion if the diffusion time is kept short enough. However, as the diffusion time is increased and more barriers hindering diffusion are encountered, the ADC will decrease (i.e. diffusion decay curves will drop off less rapidly) and reach an asymptotic value. Given the complexity and variety of published studies on restricted diffusion in tissue, the focus here will be on those measurements in nerve or white matter. The evaluation of restricted diffusion ought to better characterize the barriers to diffusion and the source of anisotropy.

In one of the first studies to address the topic of restricted diffusion in human brain white matter *in vivo*, Le Bihan *et al.* demonstrated that there was no difference in either parallel or perpendicular ADC values over diffusion times ranging from 16 to 79 ms.<sup>53</sup> Using a volume-selective, stimulated-echo technique, Horsfield *et al.* measured a dependence of the ADC on diffusion time over a larger range of diffusion times (40–800 ms) in human brain white matter *in vivo*.<sup>54</sup> However, the maximum  $b$  value used for the measured ADC values differed greatly between the shortest and longest diffusion times and notably was extraordinarily small at the shortest diffusion time of 40 ms ( $b_{\max} \sim 95 \text{ s mm}^{-2}$ ). The tensor was not used in the previous studies and fibres were chosen that were approximately aligned along the gradient axes. Clark *et al.* extended these studies on *in vivo* human brain white matter to include acquisition of the full tensor (constant  $TE$  and  $b_{\max} \sim 700 \text{ s mm}^{-2}$ ) and shorter diffusion times (8 ms).<sup>55</sup> They observed no difference in mean diffusivity, fractional anisotropy or the principal eigenvalues (although data from the most relevant eigenvalues  $\lambda_2$  and  $\lambda_3$  are not shown) over the range of diffusion times between 8 and 80 ms. The inability to measure the effects due to restricted diffusion in the above study does not mean that it is not present. As exemplified by several of the excised neural fibre work listed below, two possibilities are that the diffusion-time-dependent effects may be more apparent over a larger range of  $b$  values or that the shortest diffusion time used in this study was probably not short enough. Simulation models predict that the perpendicular ADC derived from a mono-exponential fit at low  $b$  values would start to change markedly at diffusion times less than  $\sim 4$  ms (see Fig. 3 in Szafer *et al.*<sup>56</sup> and Fig. 7 in Stanisiz *et al.*<sup>57</sup>). However, probing restricted diffusion on a clinical MRI system is inherently difficult at present since the minimum diffusion time and maximum  $b$  values are limited by the relatively weak gradients available.

Studies of excised neural fibres on NMR systems with strong gradients have yielded most of the data in terms of restriction due to the greater range of  $b$  values, the higher SNR, and the shorter attainable minimum diffusion times. Evidence of restricted diffusion in the form of diffusion-time dependency of the signal attenuation in neural fibre tracts has been reported in excised frog sciatic nerve,<sup>43,58</sup> rat sciatic nerve,<sup>39,59</sup> bovine optic nerve,<sup>57,60,61</sup> and rat spinal cord white matter.<sup>62</sup> Beaulieu and Allen demonstrated the restrictive influence of membranes perpendicular to the length of the fibre axis by substantially shortening the diffusion time from 28 ms to 2 ms in frog sciatic nerve.<sup>43</sup> The shortening of the diffusion time to 2 ms resulted in more than a two-fold increase in  $ADC(\perp)$  whereas the  $ADC(\parallel)$  remained constant, which is consistent with the assumption that relatively few barriers to diffusion exist along the length of the nerve. These alterations in the diffusion coefficients were accompanied by an equivalent decrease in the

derived anisotropy [ $ADC(\parallel)/ADC(\perp)$ ] from 5.3 at 28 ms to 2.1 at 2 ms. Even more encouraging was the agreement between the experimental frog sciatic nerve data and the model simulation results presented in Fig. 3 of the paper by Szafer *et al.*<sup>56</sup> In a study by Stanisiz *et al.*, the ADC values derived from the initial slope increased by  $<10\%$  for both the parallel and perpendicular directions when the diffusion time was decreased from 30 to 8 ms and the anisotropy did not change in the bovine optic nerve.<sup>57</sup> However, the same group demonstrated that anisotropy did decrease for the long  $T_2$  component in the same type of nerve when the diffusion time was reduced as short as 1 ms.<sup>60</sup> The differences in the signal attenuation curves with diffusion time due to restricted diffusion are more obvious, however, over a larger range of  $b$  values. Peled *et al.* reported downward shifting of the diffusion curves for the long  $T_2$  component as the diffusion time was reduced from 100 to 6 ms.<sup>58</sup> The use of the transverse relaxation property of water to try and isolate signal from individual tissue compartments will be discussed later in the article. Using  $^2\text{H}$  double-quantum-filtered NMR, Seo *et al.* have identified three water compartments due to different quadrupolar splittings in which one of those compartments, which they have assigned to intra-axonal water, demonstrated a strong dependency of the perpendicular ADC on the diffusion time.<sup>39</sup>

Assaf *et al.* have published extensively on these issues with an emphasis on q-space analysis of the diffusion data.<sup>61–63</sup> They showed that metabolites such as choline, creatine and *N*-acetyl aspartate undergo changes in the parallel and perpendicular diffusion curves as a function of diffusion time (65, 125, 245 ms) in bovine optic nerve,<sup>63</sup> in addition to water.<sup>61</sup> In a maturation study on rat spinal cord white matter, the diffusion time dependency of the perpendicular displacement profiles in immature rats indicated less hindered diffusion than in mature rats.<sup>62</sup> In summary, water diffusion is clearly restricted in neural fibre tracts such as white matter and nerve yet interpreting and relating these dependencies on diffusion time with the underlying tissue microstructural dimensions and properties is complex.

A further complicating factor in understanding the source of diffusion anisotropy in neural fibres is the fact that there are multiple distinct compartments in tissue where water can diffuse (e.g. intra-axonal, inter-axonal/extra-axonal/extra-cellular).<sup>\*</sup> The proportion of extra-cellular water in white matter/nerve is estimated to be on the order of 20–30%.<sup>65–67</sup> Identifying the properties of water, such as diffusion, in individual compartments at the microscopic level in tissue is not a trivial matter. Possible methods of obtaining NMR signal from one compartment are: (a) isolating a compartment physically

\*Although water in myelin constitutes about 15–20% of the water content, it is thought to have a very short  $T_2$  value<sup>64</sup> and hence it is typically assumed not to contribute any signal to the diffusion decay curves obtained with relatively long  $TE$ .

which only makes sense for the intra-cellular components; (b) using micro-imaging if the cell size is sufficiently large; or (c) using some other property of water (e.g.  $T_2$ ) to 'separate' the compartments (this of course uses the implicit assumption that the other NMR properties are actually identifying individual compartments themselves).

Direct measures of diffusion in the individual compartments have been reported. Intra-axonal intrinsic water diffusion with minimal interference from axonal membranes has been measured in the giant axon of the squid by Beaulieu and Allen.<sup>45</sup> Water diffusion was found to be rapid and nearly isotropic (anisotropic diffusion ratio of 1.2) in pure axoplasm. Despite the *apparently* high viscosity of axoplasm, most small ions, such as  $\text{Na}^+$  and  $\text{K}^+$ , can diffuse through axoplasm nearly as rapidly as in free solution (Rubinson and Baker<sup>68</sup> and references within). The anisotropic diffusion ratio was 1.3 for diffusion of  $^{28}\text{Mg}^{2+}$  in the squid giant axon.<sup>69</sup> The results of ion diffusion correspond well with the NMR measurements of water diffusion in axoplasm. The squid giant axon is composed of  $\sim 2.5\%$  protein and 87% water.<sup>70</sup> Surprisingly, axoplasm behaves as a fairly firm gel, and in fact, extruded axoplasm can emerge as an intact cylinder, the structural support provided by the neurofilamentary lattice.<sup>70</sup> The very small amount of protein is able to give the axoplasm a rigid mechanical strength macroscopically, but is so hydrated that the macromolecular strands are too dispersed in order to inhibit significantly the translational displacement of water or small ions. This is analogous to the near free rapid diffusion of water in agar gels.<sup>71,72</sup> Hence, the axoplasm is not as viscous, on the molecular scale, as intuition might suggest, and therefore the diffusion coefficients in pure axoplasm are not reduced to the extent that one might naively expect. Of course, as pointed out earlier, interactions of the axon water with the numerous axonal membranes in a normal neural fibre with small axons will have a marked effect in reducing the translational mobility of water relative to the free axoplasm case. In contrast to the cytoplasm of axons (i.e. axoplasm), a micro-imaging study of isolated single neurons from aplysia showed a marked reduction in ADC for water in the cytoplasm.<sup>73,74</sup> Hence, it appears that intrinsic diffusion coefficients of water in axons and neurons may differ substantially. Diffusion measurements of metabolites that are predominantly or totally in the intracellular space have shown restricted and anisotropic diffusion in bovine optic nerve.<sup>63</sup>

Extra-axonal apparent diffusion is often naively assumed to be quite free and unhindered but the data in the literature does not support that view. NMR-independent measures of anisotropy using iontophoresis of tetramethylammonium ( $\text{TMA}^+$ ) combined with ion-selective microelectrodes have shown anisotropic diffusion in the extracellular space of turtle cerebellum, rat spinal cord white matter, and rat corpus callosum.<sup>65-67</sup> It

should be borne in mind, however, that diffusion measurements using  $\text{TMA}^+$  ions probe a much longer length than the NMR measurements. Although not specific to white matter,  $^{19}\text{F}$  NMR studies by Duong *et al.* have shown that the intra- and extracellular ADC values of a compartment specific marker, 2FDG-6P, are the same in rat brain.<sup>75</sup> They confirmed that other 'extracellular' markers had similar ADC to intracellular metabolites with comparable hydrodynamic radius in rat brain.<sup>76</sup> The assumption in the previous studies, of course, is that water might behave similarly in the extracellular space. Taking the garfish nerves as an example, the root-mean-square (RMS) displacements are approximated to be  $\sim 4.5\ \mu\text{m}$  perpendicular to the long axis of the nerves over a diffusion time of 28 ms.<sup>34</sup> Numerous densely packed membrane barriers would be encountered and would hinder diffusing extra-axonal water molecules because the observed RMS is larger than typical separations between individual barriers (e.g.  $\sim 1\ \mu\text{m}$  between myelin sheaths of adjacent axons in myelinated fibres). Hence, anisotropic diffusion of water in the extra-axonal space is not an unreasonable expectation.

Others have inferred diffusion measurements in individual compartments of water in neural fibres on the basis of other NMR properties such as  $T_2$ <sup>58,60,63,77,78</sup> or quadrupolar splittings<sup>39</sup> which are assumed to differ between the compartments. Multiple  $T_2$  components are observed in nerve and white matter and they are often assigned to individual water compartments (see review by Fenrich *et al.*<sup>79</sup> and references within). Parallel ADC, perpendicular ADC, and their anisotropy were independent of spin-echo time (70–450 ms) in the *in vitro* olfactory, trigeminal and optic nerves of the garfish.<sup>77</sup> This was interpreted that the various microenvironments provided by the packed, parallel membrane structures of the axonal system give rise to similar diffusion properties in the intra- and extra-axonal spaces in nerve. In contrast, Does and Gore demonstrated an increase in parallel ADC, a decrease in perpendicular ADC, and an increase in anisotropy in the rat trigeminal nerve *in vivo* as a function of  $TE$  over 25–185 ms.<sup>78</sup> In the context of the assignment of the long-lived  $T_2$  component to extracellular water, they argue that diffusional anisotropy is greater outside than within the axons. Assaf *et al.* also showed in excised bovine optic nerve that the diffusion attenuation curves decayed more slowly as the  $TE$  was increased from 70 to 550 ms suggesting that longer  $T_2$  components had decreased diffusion properties.<sup>63</sup> Using a more sophisticated approach by measuring the  $T_2$  spectrum obtained while varying the diffusion-weighting, Stanisiz *et al.* reported anisotropy in the long  $T_2$  component ( $\sim 150$  ms) whereas the shorter  $T_2$  component ( $\sim 15$  ms) was relatively isotropic in the bovine optic nerve.<sup>60</sup> Peled *et al.*, who observed three  $T_2$  components in frog sciatic nerve, showed unique diffusion attenuation curves for the individual  $T_2$

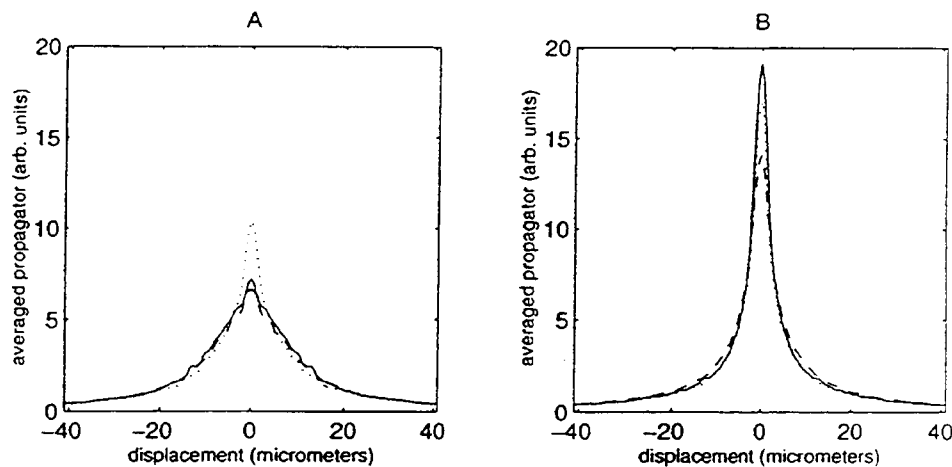


**Figure 8.**  $q$ -Space representations of probabilities of water displacements (A) parallel and (B) perpendicular to the long axis in the non-myelinated olfactory (solid line), myelinated trigeminal (dashed), and myelinated optic (dotted) nerves of the garfish. As expected for anisotropic diffusion, greater displacements are observed in the parallel direction than in the perpendicular direction. The displacement profiles are remarkably similar in these three unique nerves despite their considerable microstructural differences. Figures have been adapted from data presented in Beaulieu<sup>3</sup>

components.<sup>58</sup> Their long  $T_2$  component ( $\sim 300$  ms) showed a marked dependence on diffusion time and hence was attributed, at least in part, to intracellular water. Seo *et al.* used deuterium double quantum-filtered NMR to isolate three different compartments based on unique quadrupolar splittings in rat sciatic nerve immersed in  $D_2O$ .<sup>39</sup> One of the components demonstrated a marked dependence of the ADC on diffusion time and was attributed to axon water. Although the afore-mentioned studies provide interesting data in an attempt to measure individual diffusion properties in specific water compartments in a variety of neural fibres, it is fair to say that their interpretations are not straightforward nor conclusive at this point.

As mentioned earlier, the signal attenuation due to increasing diffusion sensitisation is anisotropic (i.e. varies with direction) over a large range of  $b$  values (Figs 5 and 7). By using very strong gradients ( $>1000$  mT  $m^{-1}$ ), marked non-monoexponential behaviour in neural fibres was first reported in five different excised garfish and bovine nerves/white matter while varying the diffusion gradient strength and keeping the diffusion time constant.<sup>34,49</sup> Examples of three of these initially reported curves from garfish are seen in Fig. 5 and agree with new data on the non-myelinated walking leg nerve of the lobster shown in Fig. 7. On the other hand, monoexponential behaviour is seen in a single component devoid of restrictive effects, such as the giant axon of the squid.<sup>45</sup> The non-monoexponential signal attenuation of the diffusion curves has subsequently been confirmed in other neural fibres such as the rat sciatic nerve,<sup>80</sup> bovine optic nerve,<sup>57,60,61</sup> frog sciatic nerve,<sup>58</sup> rat spinal cord white matter,<sup>62,81</sup> and human brain white matter.<sup>82–85</sup> The

degree of curvature and the signal amplitude at which the curves level off are typically greater for neural fibres than for grey matter in the rat brain<sup>86–89</sup> or human brain.<sup>82–85</sup>

Theoretically, deviations from linearity in a semi-log plot of signal amplitude vs  $b$  value could be due to multiple, slowly exchanging compartments with unique diffusion coefficients or restricted diffusion even in single component samples.<sup>90–92</sup> Recent interpretations of diffusion data in neural fibres by several groups whose analysis schemes have typically used bi-exponential fitting of the curves have favoured the former hypothesis.<sup>81–86,88</sup> As discussed below, when the data is taken over an even larger range of  $b$  values, bi-exponential fits are no longer adequate to fit the diffusion curves in neural tissue, and it becomes exceedingly difficult to arbitrarily assign fitted components to individual compartments like intra- and extracellular space. In fact, simulations have shown that non-monoexponential behaviour of the diffusion attenuation curves could be due to a wide range of axon sizes in the neural fibres.<sup>58</sup>

The diffusion decay curves (both parallel and perpendicular) of the three garfish nerves (Fig. 5) could often be fitted to three exponentials with  $D$  values of approximately  $1 \times 10^{-5}$ ,  $0.15 \times 10^{-5}$  and  $0.010 \times 10^{-5}$   $cm^2 s^{-1}$  with similar relative fractions for all three nerve types, whereas bi-exponential fits were not sufficient over the large range of  $b$  values (unpublished results<sup>3</sup>). In support of our unpublished observations, fitting of the multi-exponential diffusion decay curves over a large range of  $b$  values in rat brain yielded three component  $D$  values similar to the garfish nerve study.<sup>88</sup> The similarity between the three distinct garfish nerves precluded a correlation between the number of diffusion components

and the identifiable individual water compartments, as is often performed with  $T_2$  analyses of nerve.<sup>79</sup> To evaluate whether or not there was additional information (i.e. about water compartmentation) in the diffusion curves of the garfish nerves (Fig. 5), the diffusion data was processed to yield  $\mathbf{q}$ -space distributions of the particle displacements.<sup>93</sup> The original diffusion decay curves (32 data points) were interpolated to yield equally spaced data points with respect to  $\mathbf{q}$ , zero-padded to 256 data points, and then Fourier transformed to yield the displacement probabilities (Fig. 8). Although the parallel displacement profiles are certainly different from the perpendicular displacement profiles, the displacement profiles in  $\mathbf{q}$ -space are very similar for all three nerves, and therefore,  $\mathbf{q}$ -space did not aid in discriminating between the nerves nor did it provide any unique physical parameters despite their marked differences in microstructure. Others, however, have found  $\mathbf{q}$ -space analysis of neural tissue to be useful for characterizing their data.<sup>61–63,94,95</sup>

In the opinion of this author, and understanding that this is a controversial endeavour, a summary of the current 'top 10' arguments that favour the hypothesis of restricted diffusion over multicompartimentation as the *primary* source of curvature in the signal attenuation diffusion curves as a function of  $b$  value are: (1) restricted diffusion is known to occur in neural fibres; (2) marked curvatures are observed in single component systems with restriction; (3) measured populations of diffusion components in all of the reported studies don't match up with the expected microcompartments; (4) the data at higher  $b$  values requires at least three exponentials for an adequate fit rather than two; (5) diffusion attenuation curves were still non-monoexponential even when they were 'isolated' for individual  $T_2$  components or metabolites which reside primarily in one compartment (intracellular); (6) the structure of neural fibres is too complex with a multitude of cell types, axon dimensions and separations, etc. to actually expect two discrete diffusing components for intra- and extracellular space; (7) although diffusion is not likely to be uniform throughout a complex neural fibre, it is intuitively unlikely that one compartment will have an ADC an order of magnitude different than another given the packed arrangement of axons; (8) it is not necessary to assume markedly different intrinsic ADC values for intra- and extracellular space to model the diffusion curves in the theoretical studies (squid studies suggest rapid intrinsic diffusion for axoplasm); (9) one would have to assume minimal exchange between the compartments; and finally (10) changes in the diffusion curves occur with diffusion time. While it is true that fitting the data phenomenologically to multi-exponentials yields a better fit to the measured data, the resultant values do not relate, as Norris pointed out,<sup>96</sup> to any physiological compartments and furthermore, it is questionable at this stage whether this additional parametrization results in a

less ambiguous and more meaningful interpretation of diffusion in neural tissues.

## ANISOTROPY—INSIGHT FROM PATHOLOGICAL MODELS

### Demyelination and axonal degradation

Since the initial demonstrations of diffusion-weighted imaging in the nervous system, there has been hope that diffusion would provide diagnostic and physiological information that was not attainable with conventional MRI techniques, such as in the case of acute stroke. Although changes were clearly expected, the value of using measures of diffusion anisotropy as a marker for underlying tissue damage needed to be evaluated in nerve and in white matter of brain and spinal cord. A clearer association between the degree of anisotropic water diffusion and the underlying microstructural elements causing anisotropy can be better ascertained in model systems involving fibre degradation, e.g. traumatic injury, Wallerian degeneration or demyelination. This portion of the article will focus on just a few basic studies and not cover the comprehensive clinical literature in this area since it is covered in greater detail by others in this Special Issue.

Reductions in diffusion anisotropy have been shown in injury models of spinal cord white matter in rat<sup>97–99</sup> and peripheral sciatic nerves of frog<sup>100</sup> and rat.<sup>80</sup> Ford *et al.* observed reductions in anisotropy in the lateral and dorsal white matter of excised, formalin-fixed rat spinal cord 7 days after injury by a weight drop.<sup>97</sup> Specifically, the normal anisotropy [ $ADC(\parallel)/ADC(\perp)$ ] index of  $\sim 5$  was reduced to  $\sim 1$  (i.e. isotropic) in white matter that appeared abnormal on conventional spin-echo images. Interestingly, the injured, but normal-appearing white matter on conventional spin-echo had a reduced diffusion anisotropy as well. The reduction in the parallel ADC and the concomitant increase in the transverse ADC was responsible for the reduced anisotropy in this model. Although mechanical changes in the white matter such as primary mechanical disruption of axonal cylinders and loss of continuity of myelin sheaths or secondary processes such as edema or macrophage removal of necrotic tissue were assumed to be responsible for the reduced anisotropy, it was not monitored independently by histological means. Marked decreases in anisotropy have been observed in three types of garfish nerves that have degenerated *in vitro*;<sup>34</sup> however, nerve degenerating *in vitro* is not expected to correspond to nerve degenerating *in vivo*.

Subsequently, Beaulieu *et al.* reported changes in water diffusion brought about by *in vivo* Wallerian degeneration 4 weeks after either crush- or tie-injuries in the sciatic nerve of the frog.<sup>100</sup> Wallerian degeneration is characterized by structural changes such as axonal

dissolution, followed by contraction and fragmentation of the myelin, and finally disintegration and removal of myelin and other debris by Schwann cells and macrophages. Crushing a peripheral nerve interrupts axonal continuity with the cell body and causes Wallerian degeneration distal to the crush. The crush injury permits axonal regeneration to occur whereas the tie prevents the regeneration. The injured nerves showed marked approximately 2-fold reductions in anisotropic water diffusion relative to the normal controls. In agreement with the study by Ford *et al.*,<sup>97</sup> the parallel ADC decreased and the perpendicular ADC increased with injury. The importance of measuring anisotropy for assessing Wallerian degeneration was evident in that the mean diffusivities of the normal, tie-injured, and crush-injured nerves were all quite similar. Alterations in water diffusion were interpreted relative to light and electron microscopic sections of the nerves. The membrane separations, either intra- or extra-axonal (i.e. 4–10  $\mu\text{m}$  axon diameter, 0.5–2  $\mu\text{m}$  thick myelin, 0.5–2  $\mu\text{m}$  extra-axonal separations), are much smaller than the one-dimension root-mean-square displacement of a free water molecule, namely 11  $\mu\text{m}$  over a diffusion time of 28 ms. The large 4.5-fold reduction of  $\text{ADC}(\perp)$  in normal nerve from that in free water is clearly a characterization of the structural geometry of multiple membrane structures experienced by the diffusing water molecules, whereas the mere 20% reduction of  $\text{ADC}(\parallel)$  relative to free water reflects the dearth of barriers along the length of the fibres. The micrographs show that most of the axons have either collapsed or are otherwise degraded and the myelin has collapsed, fractured, and been broken down by macrophages and Schwann cells in the injured nerves. Degradation of the microstructure was severe, and hence the previously well-packed obstructions to transverse diffusion were reduced and there were more 'open' spaces between the remaining clusters of cellular remnants (isotropic tissue structures). In contrast, obstructions to parallel diffusion increased from the breakdown of the longitudinal axonal structure and the build-up of cellular debris. The crush-injured nerve had slightly higher residual anisotropy than the tie-injured nerve, presumably due to the introduction of bundles of small, non-myelinated regenerating axons which were observed in the former case. Although the interpretation of the diffusion data is not straightforward, the comparison of histological sections with the diffusion data helps in advancing our understanding on the dependency of water diffusion on the underlying microstructure. The ability to non-invasively assess regeneration, even by a coarse grading scale, may prove useful.

Further studies have extended the earlier observations on injured neural fibre tracts. Fraidakis *et al.* demonstrated that anisotropy measured *in vivo* gradually declined closer to the point of spinal cord transection in the rat.<sup>98</sup> The progressive degradation of descending and ascending spinal cord pathways was evident on histology.

The potential of using anisotropy to evaluate new therapies for spinal cord injury was presented by Nevo *et al.* where rats treated with T cells specific to the central nervous system self-antigen myelin basic protein had significantly higher anisotropy at the site of the contusion injury and better locomotion than untreated animals.<sup>99</sup> The autoimmune T cells are thought to provide neuro-protective effects and reduce the extent of degeneration. In agreement with the earlier transection study, the degree of anisotropy gradually increased away from the site of the primary lesion. Stanisiz *et al.* extended the earlier observations on Wallerian degeneration in frog sciatic nerve to a mammalian system, the rat.<sup>80</sup> Measurements of excised nerve at multiple timepoints over 6 weeks showed that anisotropy decreased and then returned to normal in the crush-injured case (degeneration followed by regeneration), whereas the anisotropy remained below normal in the cut-injured case (irreversible nerve degeneration). As noted in their article, the parallel ADC did not show any change in their model, unlike previous studies, although the degree of anisotropy in their normal nerve preparation was lower than many other neural fibres reported in the literature.

In addition to traumatic injury, secondary white matter degeneration at chronic time points after ischemia in humans results in markedly reduced anisotropy and is attributed to Wallerian degeneration of the longitudinal fibres downstream from the primary infarct.<sup>101,102</sup> Furthermore, the largest principal diffusivity (i.e. corresponding to parallel) decreased and the intermediate and lowest principal diffusivities (i.e. corresponding to perpendicular) increased in the well-oriented fibre bundles on the affected side relative to the healthy side. The average diffusivity did not change<sup>101</sup> or increased slightly<sup>102</sup> in the secondary lesion. These observations confirm the findings of the earlier animal injury models<sup>97,100</sup> and extend them to humans. An interesting point brought up by these two studies was the difference in diffusion changes between the primary lesion and the secondary white matter lesions with Wallerian degeneration. The primary white matter lesion had a greater reduction in anisotropy, markedly increased average diffusivity, and increased (rather than decreased) diffusion parallel to the fibres relative to the secondary white matter lesions undergoing Wallerian degeneration.<sup>101,102</sup> The necrotic formation of cerebrospinal fluid-filled cystic spaces with unhindered, isotropic water diffusion is consistent with a greater reduction in anisotropy, an increased mean diffusivity, and an increased parallel diffusion in the primary lesion. Pierpaoli *et al.* also caution, and quite rightly so, that diffusion changes associated with pathology in fibre tracts that are not well-defined and not coherently-oriented are trickier to interpret.<sup>102</sup>

Experimental allergic encephalomyelitis (EAE) is considered to be a model of multiple sclerosis. EAE is characterized by regions of demyelination with relative

sparing of the axons themselves. Diffusion changes have been observed in brain white matter prior to any evidence on conventional spin-echo images in a monkey model of EAE.<sup>103</sup> The increase in water diffusion perpendicular to the internal capsule fibres could be explained, at least in part, by ion-selective microelectrode studies on EAE that suggest a decrease in extracellular tortuosity.<sup>104</sup> A thorough microscopic diffusion tensor imaging study at high field of fixed, excised spinal cord from transgenic mice that spontaneously acquire EAE demonstrated reduced anisotropy in white matter regions that appeared hyperintense on conventional imaging.<sup>105</sup> These regions correlated with areas on histological slides that were characterized by parenchymal infiltration of inflammatory cells, primary demyelination, reactive astrogliosis, and some Wallerian degeneration in areas of intense inflammation. This study also noted that the mean diffusivity (one-third of the trace) varied little in lesions and hence, unlike anisotropy, was not a sensitive marker of EAE pathology. The usage of measures of diffusion anisotropy for the characterization of lesions in multiple sclerosis patients has seen a resurgence recently.

Reduced anisotropy has been observed in other animal models with abnormal levels of myelination.<sup>38,40</sup> Significant residual, albeit lower compared to normal, anisotropy is still present in those cases where histology demonstrated preservation of axons. In summary, the loss of longitudinal order given by the underlying membrane structure, either the axonal membranes themselves and/or the myelin sheaths, in nerve and white matter fibres results in significant reductions in anisotropic water diffusion in animal models of pathology that demonstrate axonal loss and/or demyelination. This emphasizes the importance of intact membranes in creating a microstructural environment that exhibits anisotropy.

## Neurotoxicity

Methylmercury is a known potent neurotoxin, although the cellular and molecular mechanisms are not fully understood. Rats intoxicated with methylmercury have shown persistent anisotropy in the optic nerve with electron microscopy confirming reductions in neurofilaments and continued integrity of the myelin sheath.<sup>106</sup> In this study, only the parallel ADC showed any change with methylmercury treatment and in fact it nearly doubled to a value approaching that of free water, which is rather surprising. A more recent study on the effects of disruption of the axonal cytoskeleton on water diffusion in spinal cord white matter of rats treated with the neurotoxin iminodipropionitrile demonstrated a reduction of parallel ADC with no change in perpendicular ADC.<sup>107</sup> This model causes the displacement of neurofilaments to the axon periphery while microtubules move to the centre. These two neurotoxicity studies, together with the vinblastine-treated garfish nerve study men-

tioned earlier where the absolute ADCs parallel and perpendicular were both reduced but the anisotropy was preserved,<sup>34</sup> demonstrate that the ADC in neural fibres can be altered by disruption of the cytoskeleton, although the unique aspects of each neurotoxic model are not well understood.

## Ischaemia

As is well known, avoidance of the confounding effects of anisotropy is a common goal in most diffusion studies of ischaemia in the brain.<sup>16,108–112</sup> However, studies with a focus on actually measuring anisotropy in ischaemic nerve and white matter may yield a better understanding on the underlying behaviour of water diffusion in neural fibres. In two early studies, the same pattern of anisotropy was seen immediately post-mortem and after acute ischaemia in cat brain relative to normal, although the degree of anisotropy was not compared quantitatively.<sup>23,113</sup> Despite an absolute reduction by 33% of the individual ADC values with ischaemia, van Gelderen *et al.* showed that the anisotropy map showed no difference between healthy and acute ischaemic cat brain.<sup>108</sup> Two studies on deep white matter in rat brain after ischaemia<sup>114</sup> and on rat spinal cord post-mortem<sup>115</sup> have demonstrated decreases in anisotropy, although the former study is difficult to assess since the healthy anisotropy was quite low to start off with and the latter's quantification scheme is not standard. Thornton *et al.* demonstrated diminished, but persistent, anisotropy in the neonatal piglet brain after transient hypoxia-ischaemia.<sup>18</sup> Although the absolute parallel and perpendicular ADCs dropped markedly in the optic and trigeminal nerves after cardiac arrest in the rat, the degree of anisotropy remained the same.<sup>116</sup> Does and Gore saw a slight increase in anisotropy in the trigeminal nerve of the rat after cardiac arrest.<sup>78</sup> Anderson *et al.* demonstrated that osmotically induced cellular swelling in the excised rat optic nerve led to a reduction of ADC in both the parallel and perpendicular directions, and that, conversely, cellular shrinkage resulted in an increase in both ADC values.<sup>117</sup> As an aside, this study on rat optic nerve<sup>117</sup> and another by Gulani *et al.* on bullfrog sciatic nerve and spinal cord<sup>118</sup> demonstrated that ADC measurements *in vitro* did not change with either depolarization alone in the absence of cell swelling or electrical stimulation, respectively.

For the most part, persistent anisotropic water diffusion after ischaemia is observed *acutely* despite absolute reductions in the parallel and perpendicular ADCs. Reductions in ADC after ischaemia are typically associated with cellular swelling (i.e. cytotoxic edema), which results in a shift of extracellular water to intracellular water. Ebisu *et al.* demonstrated that diffusion in white matter is reduced in a triethyl tin intoxication model of cytotoxic edema whereas vaso-

genic oedema results in larger ADC values.<sup>119</sup> An increase in intracellular water with greater diffusion hindrance/restriction or an increase in tortuosity of the extracellular water are two common hypotheses behind the ADC reduction transverse to the fibre tracts. A computer simulation study by Stanisz and Henkelman places greater weight on the first hypothesis.<sup>120</sup> The reduction in the ADC of water parallel to the fibres is more difficult to identify but could involve swelling of 'isotropically' shaped glial/Schwann cells in the extra-axonal space or reduced intrinsic diffusion in the intra-axonal space due to increased viscosity (cytoskeletal breakdown) or, as some others suggest, a reduction in cytoplasmic streaming after ischaemia. Based on our current understanding of anisotropy, persistent anisotropy ought to be observed in neural fibres after acute ischaemia because the longitudinal order of the fibre tracts is not compromised; however, the finer details on understanding the diverse reported observations on anisotropy *acutely* after ischaemia (small increases, small decreases, no change) remain to be uncovered. However, as mentioned earlier, *chronic* observations of anisotropy after ischaemia have demonstrated marked decreases in anisotropy which are associated with the structural breakdown of white matter fibres.<sup>101,102,121,122</sup> The study of the ischemic brain with diffusion tensor imaging is covered in greater detail by Sotak later in this issue.<sup>123</sup>

## ANISOTROPY—INSIGHT FROM DEVELOPMENT STUDIES

Few animal studies have focussed on following changes in anisotropy with maturation. The study of maturation in rat pups has demonstrated that anisotropy in white matter develops prior to histological evidence of myelination and then continues to increase as myelin forms concurrently.<sup>36,37</sup> An interesting observation is that at some point, 5–6 weeks in this model, the degree of anisotropy levelled off and did not further increase with age despite histological evidence of continued increasing myelination. In a follow-up report on a scant two rats drawn from their earlier publication, they demonstrate that anisotropy is observed in optic fibres in 7 day rat pups with lack of myelination confirmed by electron microscopy.<sup>124</sup> Also, by treating one 10-day-old rat pup with tetrodotoxin (i.e. sodium channel blocker) intraperitoneally, the authors claim to have observed *non-structural* causes of anisotropic diffusion. However, many shortcomings to this study, including lack of quantitation, poor, noisy and inappropriate anisotropy maps, numerous inconsistencies, and the obvious lack of scientific rigour in the comparison of only one animal treated with tetrodotoxin vs one without, cast serious doubt on its conclusions. Therefore, a structural source, likely the axonal membranes, of diffusion anisotropy in

the 'pre-myelination' state ought to remain the preferred hypothesis.

Takahashi *et al.* correlated measures of diffusion anisotropy with age-dependent structural changes in the optic and trigeminal nerves of the rat.<sup>125</sup> They observed a significant increase in anisotropy from 2 weeks to 10 weeks in the optic nerve which correlated with greater myelination and more orderly, less tortuous parallel fibre bundles observed by electron microscopy. They argued that the latter rationale, rather than the former, can account for the increase in anisotropy since the parallel ADC increased significantly with maturation, whereas the perpendicular ADC did not decrease significantly. The trigeminal nerve did not show changes in anisotropy over the same maturation time presumably since its myelination and coherence ('straighter fibres') were already in place by 2 weeks. In what should be considered an incidental finding and one which was not investigated further, the anisotropy of the non-myelinated and myelinated nerves of the garfish were found to be much larger in the mature garfish used in one study<sup>43</sup> relative to the smaller, immature fish used in an earlier study.<sup>34</sup> A *q*-space analysis of excised rat spinal cord by Assaf *et al.* demonstrated quite convincingly that the displacement profile perpendicular to the white matter narrowed (i.e. molecules did not diffuse as far) as the rats matured from 3 days to 10 weeks.<sup>62</sup> Varying the diffusion time from 30 to 150 ms demonstrated that water in the immature spinal cord white matter diffuses more freely and can attain greater displacements as the diffusion time is increased, whereas water in the mature spinal cord white matter is hindered by boundaries and diffuses over similar displacements at these vastly different diffusion times.

In addition to the observation of anisotropy prior to myelination, studies of cerebral white matter development in human neonates and infants *in vivo* have shown, in general, a decrease in the mean diffusivity and an increase in the degree of anisotropy with maturation.<sup>29,41,42,126</sup> These diffusion changes are linked to the concomitant increase in myelination, reduction in brain water, the greater cohesiveness and compactness of the fibre tracts, and the reduced extra-axonal space (i.e. greater packing) as the white matter matures over time. Although it is tempting to link changes in diffusion anisotropy solely to myelination during development, the evidence in the literature indicates that it would certainly be an oversimplification and may, in many cases, be an incorrect assumption. The study of the developing brain with diffusion tensor imaging is covered in greater detail by Neil *et al.* later in this issue.<sup>127</sup>

## ANISOTROPY—INSIGHT FROM MODELLING AND COMPUTER SIMULATIONS

There have been several theoretical, analytical and numerical simulation studies on diffusion in model



biological systems that lend insight into the relationship between diffusion and some of the underlying physical properties of the tissue microstructure. The advantage of such studies is the ability to perform 'experiments' that are otherwise not possible in a complex tissue system, although the caveat is that the findings are always beset with numerous assumptions and simplifications. Without going into too much detail, the salient points from some of these publications will be highlighted as they relate to anisotropy. The reader is referred to a recent review article by Norris for more extensive coverage and greater detail.<sup>96</sup>

Latour *et al.* used packed erythrocytes as a two-compartment model system (assumed spherical cells) and pointed out that the surface-to-volume ratio of biological membranes can be related to diffusion.<sup>128</sup> They argued that, since biological membrane permeabilities are small, the dominant contribution to the effective ADC comes from diffusion pathways that go around the cells rather than those that cross cell membranes. This would suggest that a single axonal membrane is sufficient to create significant anisotropy in a non-myelinated fibre. The calculated ADC values are substantially reduced despite starting with high and equal intrinsic diffusion coefficients for the intra- and extracellular space. Szafer *et al.* modelled tissue as a periodic array of numerous rectangular cells (infinitely long in one direction in some cases) surrounded by a membrane with permeability.<sup>56</sup> The perpendicular ADC drops off quickly with increasing diffusion times (for times <10 ms) and then reaches an asymptotic value as opposed to the parallel direction which does not demonstrate such a dependency on diffusion time. Thus membranes have a significant impact on the ADC and at commonly used diffusion times the measured ADC values do not correspond to the true intrinsic diffusion coefficient. The decrease in membrane permeability has little effect on the ADC for very small compartment sizes. This brings into question the importance of additional membrane layers in the form of myelin for reducing the perpendicular ADC to a further extent. One of the morals of their story is to not oversimplify the interpretation of diffusion and remember that a number of factors changing in concert could be required to predict the observed net alteration in diffusion with a given pathology. Pfeuffer *et al.* used an analytical model with restricted intracellular diffusion at permeable boundaries and extracellular tortuosity to characterize diffusion measurements in rat brain (focus on grey matter).<sup>129</sup> In agreement with the numerous experimental observations reported earlier in the article, these three studies emphasize the importance of membranes in hindering water diffusion.

The previous three models were primarily focussed on better understanding the reductions in ADC associated with acute ischaemia. Other studies have aimed their efforts primarily on understanding diffusion specifically in neural fibres such as nerve and white matter. Beaulieu

and Allen performed Monte Carlo computer simulations of two-dimensional diffusion amongst a regular, hexagonal array of impermeable circular barriers which represent the neurofilaments present in the axoplasm.<sup>45</sup> This hexagonal array had a relatively weak influence on diffusion over an appropriate range of barrier spacings and the predicted degree of anisotropy matched well with the nearly isotropic diffusion measured in the squid giant axon [ $ADC(\parallel)/ADC(\perp) = 1.2$ ]. Together with previous studies, this work confirmed the primary role of membranes in producing diffusional anisotropy.

In a purely theoretical study, Ford *et al.* presented a numerical model to predict the alterations in the transverse ADC seen in spinal cord white matter injury as a function of axonal diameter and separation, membrane permeability, relative axonal volume and diffusion time.<sup>130,131</sup> The first paper addressed the scenario of abutting (i.e. touching) cylinders (i.e. axons), whereas the later one left a gap between adjacent cylinders to leave a contiguous extracellular space. Mild injury was modelled as an increase in intracellular water fraction to represent axonal swelling and increased permeability. They assumed that the intrinsic intracellular diffusion coefficient was  $\sim 4$  times less than the intrinsic extracellular diffusion coefficient which is likely to be a gross overestimation given that the intrinsic water diffusion in axoplasm is about 80% of that in free water.<sup>45</sup>

Nonetheless, several trends are worth noting. The perpendicular (or transverse) ADC depends on axonal diameter at short diffusion times, whereas for a given axonal separation (with different sized axons) asymptotic values of ADC are determined by permeability alone. For diffusion times greater than  $\sim 10$  ms, which is used in most cases, transverse diffusion measurements are in the asymptotic regime and it is certainly dominated by restriction. Significant numbers of water molecules will still impinge on the membranes at the shortest diffusion times attainable at present. Their results also signify that the morphology of the extracellular space, not just relative volume, is a factor in determining the transverse ADC at experimentally realizable diffusion times.

Stanisz *et al.* presented a comprehensive analytical model which was used to fit the parallel and perpendicular diffusion curves to high  $b$  values at multiple diffusion times experimentally obtained from the excised bovine optic nerve.<sup>57</sup> Axonal and glial cells are modelled as prolate ellipsoids and spheres, respectively, which are surrounded by partially permeable membranes. Their model and fitted parameters successfully described the salient characteristics of the PGSE diffusion data, namely the anisotropy, diffusion time dependence and upward curvature of the decay curves. Once again, diffusion of water in cells is highly restricted due to barriers such as cell membranes. Three compartments (spherical glial cells as well as the ellipsoid axons and extra-cellular space) and a small amount of finite permeability (as

opposed to none) were needed to properly fit the experimental data. The spherical glial cells were needed to obtain the upward curvature of the diffusion decay curves parallel to the fibre. They stress that a wide range of data at short and long diffusion times and high  $b$  values are needed to obtain meaningful model parameters from the fitted data and that the initial slope measurements of ADC do not provide a complete picture of restricted diffusion in tissue. This model presents the minimal complexity (three compartments, nine parameters) needed for a satisfactory fit to their data. The resultant microstructural parameters appear reasonable. Tests in other systems with known differences in the various parameters would help validate the model. One questionable assumption, however, is the ellipsoid shape of the axons. Axons are essentially infinitely long cylinders (over the scale of NMR measurements) and it is not known if and how this non-ellipsoid nature influences the fitted results of diffusion parallel to the fibres. As we pointed out earlier though, simplifications and assumptions are obviously necessary in modelling complex biological tissues. Stanis and Henkelman have recently used their model to predict the effects of axonal swelling on the diffusion characteristics in white matter.<sup>120</sup> Their simulations suggested that the ADC decrease from axonal swelling is mainly due to the water shift from the extracellular space into the *highly restricted* intracellular compartment whereas increased extracellular tortuosity had a smaller effect. Overall, the aforementioned theoretical, analytical and numerical studies have provided a conceptual framework from which to better understand changes in water diffusion in the nervous system and specifically demonstrate the importance of limited permeability barriers (i.e. membranes) in hindering perpendicular water diffusion and creating the anisotropy used for fibre tracking in DTI investigations.

## CONCLUSIONS

Although the interpretation of water diffusion in a complex biological tissue such as nerve and white matter is still not trivial, numerous studies over the last decade have provided a better understanding of the relationship between diffusion and the underlying microstructural components. Evidence suggests that anisotropic water diffusion in neural fibres is due to the dense packing of axons and their inherent axonal membranes that hinder water diffusion significantly perpendicular to the long axis of the fibres relative to the preferential parallel direction. By providing a further example in this review of diffusion anisotropy in a normal, non-myelinated nerve, namely the walking leg nerve of the lobster, myelin is shown once again not to be a primary determinant of anisotropy, although reports suggest that it may modulate the degree of anisotropy in a given fibre tract. Measurements of anisotropic water diffusion,

particularly for non-invasive fibre tracking, have become much more mainstream in recent years and it is hoped that the background information provided in this article is timely and informative for those interested in using and interpreting changes in this unique property of water.

## Acknowledgements

The author acknowledges the Alberta Heritage Foundation for Medical Research (AHFMR) and the Canadian Institutes of Health Research (CIHR) for financial support.

## REFERENCES

1. Moseley ME, Wendland MF, Kucharczyk J. Magnetic resonance imaging of diffusion and perfusion. *Top. Magn. Reson. Imag.* 1991; **3**: 50–67.
2. Sotak CH, Li L. MR imaging of anisotropic and restricted diffusion by simultaneous use of spin and stimulated echoes. *Magn. Reson. Med.* 1992; **26**: 174–183.
3. Beaulieu C. An NMR evaluation of water diffusion and magnetization transfer in nerve. Ph.D. thesis, Biomedical Engineering, University of Alberta, 1995.
4. Stejskal EO, Tanner JE. Spin diffusion measurements: spin echoes in the presence of a time-dependent field gradient. *J. Chem. Phys.* 1965; **42**: 288–292.
5. Basser PJ, Mattiello J, LeBihan D. Estimation of the effective self-diffusion tensor from the NMR spin echo. *J. Magn. Reson. B* 1994; **103**: 247–254.
6. Basser PJ, Mattiello J, LeBihan D. MR diffusion tensor spectroscopy and imaging. *Biophys. J.* 1994; **66**: 259–267.
7. Pierpaoli C, Basser PJ. Toward a quantitative assessment of diffusion anisotropy. *Magn. Reson. Med.* 1996; **36**: 893–906.
8. Ulug AM, van Zijl PC. Orientation-independent diffusion imaging without tensor diagonalization: anisotropy definitions based on physical attributes of the diffusion ellipsoid. *J. Magn. Reson. Imag.* 1999; **9**: 804–813.
9. Finch ED, Harmon JF, Muller BH. Pulsed NMR measurements of the diffusion constant of water in muscle. *Arch. Biochem. Biophys.* 1971; **147**: 299–310.
10. Hansen JR. Pulsed NMR study of water mobility in muscle and brain tissue. *Biochim. Biophys. Acta* 1971; **230**: 482–486.
11. Cleveland GG, Chang DC, Hazlewood CF, Rorschach HE. Nuclear magnetic resonance measurement of skeletal muscle: anisotropy of the diffusion coefficient of the intracellular water. *Biophys. J.* 1976; **16**: 1043–1053.
12. Callaghan PT. Pulsed field gradient nuclear magnetic resonance as a probe of liquid state molecular organization. *Aust. J. Phys.* 1984; **37**: 359–387.
13. Wesbey GE, Moseley ME, Ehman RL. Translational molecular self-diffusion in magnetic resonance imaging. II. Measurement of the self-diffusion coefficient. *Invest. Radiol.* 1984; **19**: 491–498.
14. Thomsen C, Henriksen O, Ring P. *In vivo* measurement of water self diffusion in the human brain by magnetic resonance imaging. *Acta Radiol.* 1987; **28**: 353–361.
15. Hoehn-Berlage M, Eis M, Back T, Kohno K, Yamashita K. Changes of relaxation times ( $T_1$ ,  $T_2$ ) and apparent diffusion coefficient after permanent middle cerebral artery occlusion in the rat: temporal evolution, regional extent, and comparison with histology. *Magn. Reson. Med.* 1995; **34**: 824–834.
16. Lythgoe MF, Busza AL, Calamante F, Sotak CH, King MD, Bingham AC, Williams SR, Gadian DG. Effects of diffusion anisotropy on lesion delineation in a rat model of cerebral ischemia. *Magn. Reson. Med.* 1997; **38**: 662–668.
17. Hoehn-Berlage M, Eis M, Schmitz B. Regional and directional anisotropy of apparent diffusion coefficient in rat brain. *NMR Biomed.* 1999; **12**: 45–50.

18. Thornton JS, Ordidge RJ, Penrice J, Cady EB, Amess PN, Punwani S, Clemence M, Wyatt JS. Anisotropic water diffusion in white and gray matter of the neonatal piglet brain before and after transient hypoxia-ischaemia. *Magn. Reson. Imag.* 1997; **15**: 433–440.
19. Chenevert TL, Brunberg JA, Pipe JG. Anisotropic diffusion in human white matter: demonstration with MR techniques in vivo. *Radiology* 1990; **177**: 401–405.
20. Chien D, Buxton RB, Kwong KK, Brady TJ, Rosen BR. MR diffusion imaging of the human brain. *J. Comput. Assist. Tomogr.* 1990; **14**: 514–520.
21. Doran M, Hajnal JV, Van Bruggen N, King MD, Young IR, Bydder GM. Normal and abnormal white matter tracts shown by MR imaging using directional diffusion weighted sequences. *J. Comput. Assist. Tomogr.* 1990; **14**: 865–873.
22. Turner R, Le Bihan D, Maier J, Vavrek R, Hedges LK, Pekar J. Echo-planar imaging of intravoxel incoherent motion. *Radiology* 1990; **177**: 407–414.
23. Moseley ME, Cohen YC, Kucharczyk J, Asgari HS, Wendland MF, Tsuruda J, Norman D. Diffusion-weighted MR imaging of anisotropic water diffusion in cat central nervous system. *Radiology* 1990; **176**: 439–445.
24. Hajnal JV, Doran M, Hall AS, Collins AG, Oatridge A, Pennock JM, Young IR, Bydder GM. MR imaging of anisotropically restricted diffusion of water in the nervous system: technical, anatomic, and pathologic considerations. *J. Comput. Assist. Tomogr.* 1991; **15**: 1–18.
25. Moseley ME, Kucharczyk J, Asgari HS, Norman D. Anisotropy in diffusion-weighted MRI. *Magn. Reson. Med.* 1991; **19**: 321–326.
26. Howe FA, Filler AG, Bell BA, Griffiths JR. Magnetic resonance neurography. *Magn. Reson. Med.* 1992; **28**: 328–338.
27. King MD, van Bruggen N, Ahier RG, Cremer JE, Hajnal JV, Williams SR, Doran M. Diffusion-weighted imaging of kainic acid lesions in the rat brain. *Magn. Reson. Med.* 1991; **20**: 158–164.
28. Rutherford MA, Cowan FM, Manzur AY, Dubowitz LM, Pennock JM, Hajnal JV, Young IR, Bydder GM. MR imaging of anisotropically restricted diffusion in the brain of neonates and infants. *J. Comput. Assist. Tomogr.* 1991; **15**: 188–198.
29. Sakuma H, Nomura Y, Takeda K, Tagami T, Nakagawa T, Tamagawa Y, Ishii Y, Tsukamoto T. Adult and neonatal human brain: diffusional anisotropy and myelination with diffusion-weighted MR imaging. *Radiology* 1991; **180**: 229–233.
30. Douek P, Turner R, Pekar J, Patronas N, Le Bihan D. MR color mapping of myelin fiber orientation. *J. Comput. Assist. Tomogr.* 1991; **15**: 923–929.
31. Le Bihan D. Molecular diffusion nuclear magnetic resonance imaging. *Magn. Reson. Q.* 1991; **7**: 1–30.
32. Hong X, Dixon WT. Measuring diffusion in inhomogeneous systems in imaging mode using antisymmetric sensitizing gradients. *J. Magn. Reson.* 1992; **99**: 561–570.
33. Lian J, Williams DS, Lowe IJ. Magnetic resonance imaging of diffusion in the presence of background gradients and imaging of background gradients. *J. Magn. Reson. A* 1994; **106**: 65–74.
34. Beaulieu C, Allen PS. Determinants of anisotropic water diffusion in nerves. *Magn. Reson. Med.* 1994; **31**: 394–400.
35. Darin De Lorenzo AJ, Brzin M, Dettbarn WD. Fine structure and organization of nerve fibers and giant axons in *Homarus americanus*. *J. Ultrastruct. Res.* 1968; **24**: 367–384.
36. Wimberger DM, Roberts TP, Barkovich AJ, Prayer LM, Moseley ME, Kucharczyk J. Identification of “premyelination” by diffusion-weighted MRI. *J. Comput. Assist. Tomogr.* 1995; **19**: 28–33.
37. Prayer D, Roberts T, Barkovich AJ, Prayer L, Kucharczyk J, Moseley M, Arieff A. Diffusion-weighted MRI of myelination in the rat brain following treatment with gonadal hormones. *Neuroradiology* 1997; **39**: 320–325.
38. Ono J, Harada K, Takahashi M, Maeda M, Ikenaka K, Sakurai K, Sakai N, Kagawa T, Fritz-Zieroth B, Nagai T *et al.* Differentiation between dysmyelination and demyelination using magnetic resonance diffusional anisotropy. *Brain Res.* 1995; **671**: 141–148.
39. Seo Y, Shinar H, Morita Y, Navon G. Anisotropic and restricted diffusion of water in the sciatic nerve: A (2)H double-quantum-filtered NMR study. *Magn. Reson. Med.* 1999; **42**: 461–466.
40. Gulani V, Webb AG, Duncan ID, Lauterbur PC. Apparent diffusion tensor measurements in myelin-deficient rat spinal cords. *Magn. Reson. Med.* 2001; **45**: 191–195.
41. Huppi PS, Maier SE, Peled S, Zientara GP, Barnes PD, Jolesz FA, Volpe JJ. Microstructural development of human newborn cerebral white matter assessed in vivo by diffusion tensor magnetic resonance imaging. *Pediatr. Res.* 1998; **44**: 584–590.
42. Neil JJ, Shiran SI, McKinstry RC, Schefft GL, Snyder AZ, Almlí CR, Akbudak E, Aronovitz JA, Miller JP, Lee BC, Conturo TE. Normal brain in human newborns: apparent diffusion coefficient and diffusion anisotropy measured by using diffusion tensor MR imaging. *Radiology* 1998; **209**: 57–66.
43. Beaulieu C, Allen PS. An in vitro evaluation of the effects of local magnetic-susceptibility-induced gradients on anisotropic water diffusion in nerve. *Magn. Reson. Med.* 1996; **36**: 39–44.
44. Pierpaoli C, Jezzard P, Basser PJ, Barnett A, Di Chiro G. Diffusion tensor MR imaging of the human brain. *Radiology* 1996; **201**: 637–648.
45. Beaulieu C, Allen PS. Water diffusion in the giant axon of the squid: implications for diffusion-weighted MRI of the nervous system. *Magn. Reson. Med.* 1994; **32**: 579–583.
46. Trudeau JD, Dixon WT, Hawkins J. The effect of inhomogeneous sample susceptibility on measured diffusion anisotropy using NMR imaging. *J. Magn. Reson. B* 1995; **108**: 22–30.
47. Clark CA, Barker GJ, Tofts PS. An in vivo evaluation of the effects of local magnetic susceptibility-induced gradients on water diffusion measurements in human brain. *J. Magn. Reson.* 1999; **141**: 52–61.
48. Menzel MI, Han SI, Stapf S, Blumich B. NMR characterization of the pore structure and anisotropic self-diffusion in salt water ice. *J. Magn. Reson.* 2000; **143**: 376–381.
49. Henkelman RM, Stanisz GJ, Kim JK, Bronskill MJ. Anisotropy of NMR properties of tissues. *Magn. Reson. Med.* 1994; **32**: 592–601.
50. Garrido L, Wedeen VJ, Kwong KK, Spencer UM, Kantor HL. Anisotropy of water diffusion in the myocardium of the rat. *Circul. Res.* 1994; **74**: 789–793.
51. Cooper RL, Chang DB, Young AC, Martin CJ, Ancker-Johnson D. Restricted diffusion in biophysical systems. *Experiment. Biophys. J.* 1974; **14**: 161–177.
52. Karger J, Pfeifer H, Heink W. Principles and application of self-diffusion measurements by nuclear magnetic resonance. In *Advances in Magnetic Resonance*, Waugh JS (ed.). Academic Press: San Diego, CA, 1988; 1–89.
53. Le Bihan D, Turner R, Douek P. Is water diffusion restricted in human brain white matter? An echo-planar NMR imaging study. *Neuroreport* 1993; **4**: 887–890.
54. Horsfield MA, Barker GJ, McDonald WI. Self-diffusion in CNS tissue by volume-selective proton NMR. *Magn. Reson. Med.* 1994; **31**: 637–644.
55. Clark CA, Hedehus M, Moseley ME. Diffusion time dependence of the apparent diffusion tensor in healthy human brain and white matter disease. *Magn. Reson. Med.* 2001; **45**: 1126–1129.
56. Szafer A, Zhong J, Gore JC. Theoretical model for water diffusion in tissues. *Magn. Reson. Med.* 1995; **33**: 697–712.
57. Stanisz GJ, Szafer A, Wright GA, Henkelman RM. An analytical model of restricted diffusion in bovine optic nerve. *Magn. Reson. Med.* 1997; **37**: 103–111.
58. Peled S, Cory DG, Raymond SA, Kirschner DA, Jolesz FA. Water diffusion, T<sub>2</sub>, and compartmentation in frog sciatic nerve. *Magn. Reson. Med.* 1999; **42**: 911–918.
59. Seo Y, Morita Y, Kusaka Y, Steward MC, Murakami M. Diffusion of water in rat sciatic nerve measured by 1H pulsed field gradient NMR: compartmentation and anisotropy. *Jpn. J. Physiol.* 1996; **46**: 163–169.
60. Stanisz GJ, Henkelman RM. Diffusional anisotropy of T<sub>2</sub> components in bovine optic nerve. *Magn. Reson. Med.* 1998; **40**: 405–410.
61. Assaf Y, Cohen Y. Assignment of the water slow-diffusing component in the central nervous system using q-space diffusion MRS: implications for fiber tract imaging. *Magn. Reson. Med.* 2000; **43**: 191–199.
62. Assaf Y, Mayk A, Cohen Y. Displacement imaging of spinal cord using q-space diffusion-weighted MRI. *Magn. Reson. Med.* 2000; **44**: 713–722.

63. Assaf Y, Cohen Y. Structural information in neuronal tissue as revealed by q-space diffusion NMR spectroscopy of metabolites in bovine optic nerve. *NMR Biomed.* 1999; **12**: 335–344.
64. MacKay A, Whittall K, Adler J, Li D, Paty D, Graeb D. In vivo visualization of myelin water by magnetic resonance. *Magn. Reson. Med.* 1994; **31**: 673–677.
65. Rice ME, Okada YC, Nicholson C. Anisotropic and heterogeneous diffusion in the turtle cerebellum: implications for volume transmission. *J. Neurophysiol.* 1993; **70**: 2035–2044.
66. Vorisek I, Sykova E. Evolution of anisotropic diffusion in the developing rat corpus callosum. *J. Neurophysiol.* 1997; **78**: 912–919.
67. Sykova E, Vargova L, Prokopova S, Simonova Z. Glial swelling and astroglial produce diffusion barriers in the rat spinal cord. *Glia* 1999; **25**: 56–70.
68. Rubinson KA, Baker PF. The flow properties of axoplasm in a defined chemical environment: influence of anions and calcium. *Proc. R. Soc. Lond. B Biol. Sci.* 1979; **205**: 323–345.
69. Baker PF, Crawford AC. Mobility and transport of magnesium in squid giant axons. *J. Physiol.* 1972; **227**: 855–874.
70. Brown A, Lasek RJ. The cytoskeleton of the squid giant axon. In *Squid as Experimental Animals*, Adelman WJ, Gilbert DL, Arnold JM (eds). Plenum Press: New York, 1990; 235–302.
71. Woessner DE, Snowden BS, Chiu YC. Pulsed NMR study of the temperature hysteresis in the agar–water system. *J. Colloid Interface Sci.* 1970; **34**: 283–289.
72. Derbyshire W, Duff ID. NMR of agarose gels. *Faraday Disc. Chem. Soc.* 1974; **57**: 243–254.
73. Schoeniger JS, Aiken N, Hsu E, Blackband SJ. Relaxation-time and diffusion NMR microscopy of single neurons. *J. Magn. Reson. B* 1994; **103**: 261–273.
74. Hsu EW, Aiken NR, Blackband SJ. A study of diffusion isotropy in single neurons by using NMR microscopy. *Magn. Reson. Med.* 1997; **37**: 624–627.
75. Duong TQ, Ackerman JJ, Ying HS, Neil JJ. Evaluation of extra- and intracellular apparent diffusion in normal and globally ischemic rat brain via 19F NMR. *Magn. Reson. Med.* 1998; **40**: 1–13.
76. Duong TQ, Sehy JV, Yablonskiy DA, Snider BJ, Ackerman JJ, Neil JJ. Extracellular apparent diffusion in rat brain. *Magn. Reson. Med.* 2001; **45**: 801–810.
77. Beaulieu C, Fenrich FR, Allen PS. Multicomponent water proton transverse relaxation and T2-discriminated water diffusion in myelinated and nonmyelinated nerve. *Magn. Reson. Imag.* 1998; **16**: 1201–1210.
78. Does MD, Gore JC. Compartmental study of diffusion and relaxation measured in vivo in normal and ischemic rat brain and trigeminal nerve. *Magn. Reson. Med.* 2000; **43**: 837–844.
79. Fenrich FR, Beaulieu C, Allen PS. Relaxation times and microstructures. *NMR Biomed.* 2001; **14**: 133–139.
80. Stanis GJ, Midha R, Munro CA, Henkelman RM. MR properties of rat sciatic nerve following trauma. *Magn. Reson. Med.* 2001; **45**: 415–420.
81. Inglis BA, Bossart EL, Buckley DL, Wirth ED III, Mareci TH. Visualization of neural tissue water compartments using biexponential diffusion tensor MRI. *Magn. Reson. Med.* 2001; **45**: 580–587.
82. Mulkern RV, Gudbjartsson H, Westin CF, Zengingonul HP, Gartner W, Guttman CR, Robertson RL, Kyriakos W, Schwartz R, Holtzman D, Jolesz FA, Maier SE. Multi-component apparent diffusion coefficients in human brain. *NMR Biomed.* 1999; **12**: 51–62.
83. Mulkern RV, Zengingonul HP, Robertson RL, Bogner P, Zou KH, Gudbjartsson H, Guttman CR, Holtzman D, Kyriakos W, Jolesz FA, Maier SE. Multi-component apparent diffusion coefficients in human brain: relationship to spin-lattice relaxation. *Magn. Reson. Med.* 2000; **44**: 292–300.
84. Clark CA, Le Bihan D. Water diffusion compartmentation and anisotropy at high *b* values in the human brain. *Magn. Reson. Med.* 2000; **44**: 852–859.
85. Yoshiura T, Wu O, Zaheer A, Reese TG, Sorensen AG. Highly diffusion-sensitized MRI of brain: Dissociation of gray and white matter. *Magn. Reson. Med.* 2001; **45**: 734–740.
86. Niendorf T, Dijkhuizen RM, Norris DG, van Lookeren Campagne M, Nicolay K. Biexponential diffusion attenuation in various states of brain tissue: implications for diffusion-weighted imaging. *Magn. Reson. Med.* 1996; **36**: 847–857.
87. Assaf Y, Cohen Y. Non-mono-exponential attenuation of water and N-acetyl aspartate signals due to diffusion in brain tissue. *J. Magn. Reson.* 1998; **131**: 69–85.
88. Pfeuffer J, Provencher SW, Gruetter R. Water diffusion in rat brain in vivo as detected at very large *b* values is multi-compartmental. *Magma* 1999; **8**: 98–108.
89. Buckley DL, Bui JD, Phillips MI, Zelles T, Inglis BA, Plant HD, Blackband SJ. The effect of ouabain on water diffusion in the rat hippocampal slice measured by high resolution NMR imaging. *Magn. Reson. Med.* 1999; **41**: 137–142.
90. Zhong JH, Gore JC. Studies of restricted diffusion in heterogeneous media containing variations in susceptibility. *Magn. Reson. Med.* 1991; **19**: 276–284.
91. Hürlimann MD, Helmer KG, de Swiet TM, Sen PN, Sotak CH. Spin echoes in a constant gradient and in the presence of simple restriction. *J. Magn. Reson. A* 1995; **113**: 260–264.
92. Helmer KG, Dardzinski BJ, Sotak CH. The application of porous-media theory to the investigation of time-dependent diffusion in vivo systems. *NMR Biomed.* 1995; **8**: 297–306.
93. Cory DG, Garroway AN. Measurement of translational displacement probabilities by NMR: an indicator of compartmentation. *Magn. Reson. Med.* 1990; **14**: 435–444.
94. King MD, Houseman J, Roussel SA, van Bruggen N, Williams SR, Gadian DG. q-Space imaging of the brain. *Magn. Reson. Med.* 1994; **32**: 707–713.
95. King MD, Houseman J, Gadian DG, Connelly A. Localized q-space imaging of the mouse brain. *Magn. Reson. Med.* 1997; **38**: 930–937.
96. Norris DG. The effects of microscopic tissue parameters on the diffusion weighted magnetic resonance imaging experiment. *NMR Biomed.* 2001; **14**: 77–93.
97. Ford JC, Hackney DB, Alsop DC, Jara H, Joseph PM, Hand CM, Black P. MRI characterization of diffusion coefficients in a rat spinal cord injury model. *Magn. Reson. Med.* 1994; **31**: 488–494.
98. Fraidakis M, Klason T, Cheng H, Olson L, Spenger C. High-resolution MRI of intact and transected rat spinal cord. *Exp. Neurol.* 1998; **153**: 299–312.
99. Nevo U, Hauben E, Yoles E, Agranov E, Akselrod S, Schwartz M, Neeman M. Diffusion anisotropy MRI for quantitative assessment of recovery in injured rat spinal cord. *Magn. Reson. Med.* 2001; **45**: 1–9.
100. Beaulieu C, Does MD, Snyder RE, Allen PS. Changes in water diffusion due to Wallerian degeneration in peripheral nerve. *Magn. Reson. Med.* 1996; **36**: 627–631.
101. Werring DJ, Toosy AT, Clark CA, Parker GJ, Barker GJ, Miller DH, Thompson AJ. Diffusion tensor imaging can detect and quantify corticospinal tract degeneration after stroke. *J. Neurol. Neurosurg. Psychiat.* 2000; **69**: 269–272.
102. Pierpaoli C, Barnett A, Pajevic S, Chen R, Penix L, Virta A, Basser P. Water diffusion changes in wallerian degeneration and their dependence on white matter architecture. *Neuroimage* 2001; **13**: 1174–1185.
103. Heide AC, Richards TL, Alvord EC Jr, Peterson J, Rose LM. Diffusion imaging of experimental allergic encephalomyelitis. *Magn. Reson. Med.* 1993; **29**: 478–484.
104. Simonova Z, Svoboda J, Orkand P, Bernard CC, Lassmann H, Sykova E. Changes of extracellular space volume and tortuosity in the spinal cord of Lewis rats with experimental autoimmune encephalomyelitis. *Physiol. Res.* 1996; **45**: 11–22.
105. Ahrens ET, Laidlaw DH, Readhead C, Brosnan CF, Fraser SE, Jacobs RE. MR microscopy of transgenic mice that spontaneously acquire experimental allergic encephalomyelitis. *Magn. Reson. Med.* 1998; **40**: 119–132.
106. Kinoshita Y, Ohnishi A, Kohshi K, Yokota A. Apparent diffusion coefficient on rat brain and nerves intoxicated with methylmercury. *Environ. Res.* 1999; **80**: 348–354.
107. Shepherd TM, Thelwall PE, Wirth ED. Non-lethal disruption of the axonal cytoskeleton alters water diffusion in spinal cord white matter. In *Proceedings of the 9th ISMRM*, Glasgow, Scotland, 2001; 1624.
108. van Gelderen P, de Vleeschouwer MH, DesPres D, Pekar J, van Zijl PC, Moonen CT. Water diffusion and acute stroke. *Magn. Reson. Med.* 1994; **31**: 154–163.

109. Wong EC, Cox RW, Song AW. Optimized isotropic diffusion weighting. *Magn. Reson. Med.* 1995; **34**: 139–143.
110. Mori S, van Zijl PC. Diffusion weighting by the trace of the diffusion tensor within a single scan. *Magn. Reson. Med.* 1995; **33**: 41–52.
111. Butts K, Pauly J, de Crespigny A, Moseley M. Isotropic diffusion-weighted and spiral-navigated interleaved EPI for routine imaging of acute stroke. *Magn. Reson. Med.* 1997; **38**: 741–749.
112. Ulug AM, Beauchamp N, Jr., Bryan RN, van Zijl PC. Absolute quantitation of diffusion constants in human stroke. *Stroke* 1997; **28**: 483–490.
113. Moonen CT, Pekar J, de Vleeschouwer MH, van Gelderen P, van Zijl PC, DesPres D. Restricted and anisotropic displacement of water in healthy cat brain and in stroke studied by NMR diffusion imaging. *Magn. Reson. Med.* 1991; **19**: 327–332.
114. Kajima T, Azuma K, Itoh K, Kagawa R, Yamane K, Okada Y, Shima T. Diffusion anisotropy of cerebral ischaemia. *Acta Neurochir. Suppl.* 1994; **60**: 216–219.
115. Matsuzawa H, Kwee IL, Nakada T. Magnetic resonance axonography of the rat spinal cord: postmortem effects. *J. Neurosurg.* 1995; **83**: 1023–1028.
116. Beaulieu C, Busch E, de Crespigny A, Rother J, Moseley ME. Water diffusion in the optic and trigeminal nerve after cardiac arrest in the rat. In *Proceedings of the 5th ISMRM*, Vancouver, BC, 1997; 613.
117. Anderson AW, Zhong J, Petroff OA, Szafer A, Ransom BR, Prichard JW, Gore JC. Effects of osmotically driven cell volume changes on diffusion-weighted imaging of the rat optic nerve. *Magn. Reson. Med.* 1996; **35**: 162–167.
118. Gulani V, Iwamoto GA, Lauterbur PC. Apparent water diffusion measurements in electrically stimulated neural tissue. *Magn. Reson. Med.* 1999; **41**: 241–246.
119. Ebisu T, Naruse S, Horikawa Y, Ueda S, Tanaka C, Uto M, Umeda M, Higuchi T. Discrimination between different types of white matter edema with diffusion-weighted MR imaging. *J. Magn. Reson. Imag.* 1993; **3**: 863–868.
120. Stanisz G, Henkelman RM. Effects of cellular swelling on diffusion in white matter. In *Proceedings of the 9th ISMRM*, Glasgow, Scotland, 2001; 350.
121. Makris N, Worth AJ, Sorensen AG, Papadimitriou GM, Wu O, Reese TG, Wedeen VJ, Davis TL, Stakes JW, Caviness VS, Kaplan E, Rosen BR, Pandya DN, Kennedy DN. Morphometry of in vivo human white matter association pathways with diffusion-weighted magnetic resonance imaging. *Ann. Neurol.* 1997; **42**: 951–962.
122. Beaulieu C, Moseley ME. Diffusion-weighted and perfusion-weighted magnetic resonance imaging in clinical stroke. In *Current Review of Cerebrovascular Disease*, Fisher M, Bogouslavsky J (eds). Current Medicine: Philadelphia, PA, 1999; 53–64.
123. Sotak CH. The role of diffusion tensor imaging (DTI) in the evaluation of ischemic brain injury. *NMR Biomed.* 2002; **17**: 561–565.
124. Prayer D, Barkovich AJ, Kirschner DA, Prayer LM, Roberts TP, Kucharczyk J, Moseley ME. Visualization of nonstructural changes in early white matter development on diffusion-weighted mr images: evidence supporting premyelination anisotropy. *Am. J. Neuroradiol.* 2001; **22**: 1572–1576.
125. Takahashi M, Ono J, Harada K, Maeda M, Hackney DB. Diffusional anisotropy in cranial nerves with maturation: quantitative evaluation with diffusion MR imaging in rats. *Radiology* 2000; **216**: 881–885.
126. Nomura Y, Sakuma H, Takeda K, Tagami T, Okuda Y, Nakagawa T. Diffusional anisotropy of the human brain assessed with diffusion-weighted MR: relation with normal brain development and aging. *Am. J. Neuroradiol.* 1994; **15**: 231–238.
127. Neil J, Miller J, Huppi PS. Diffusion tensor imaging of the developing human brain. *NMR Biomed.* 2002; **17**: 543–550.
128. Latour LL, Svoboda K, Mitra PM, Sotak CH. Time-dependent diffusion of water in a biological model system. *Proc. Natl Acad. Sci.* 1994; **91**: 1229–1233.
129. Pfeuffer J, Dreher W, Sykova E, Leibfritz D. Water signal attenuation in diffusion-weighted <sup>1</sup>H NMR experiments during cerebral ischemia: influence of intracellular restrictions, extracellular tortuosity, and exchange. *Magn. Reson. Imag.* 1998; **16**: 1023–1032.
130. Ford JC, Hackney DB. Numerical model for calculation of apparent diffusion coefficients (ADC) in permeable cylinders—comparison with measured ADC in spinal cord white matter. *Magn. Reson. Med.* 1997; **37**: 387–394.
131. Ford JC, Hackney DB, Lavi E, Phillips M, Patel U. Dependence of apparent diffusion coefficients on axonal spacing, membrane permeability, and diffusion time in spinal cord white matter. *J. Magn. Reson. Imag.* 1998; **8**: 775–782.